NASA Contractor Report 163104

NASA-CR-163104
19810008436

AN INVESTIGATION OF DRAG REDUCTION FOR TRACTOR TRAILER VEHICLES WITH AIR DEFLECTOR AND BOATTAIL

Vincent U. Muirhead

Contract NSG 4021 and 4023
January 1981

NASA

NF02058

NASA Contractor Report 163104

AN INVESTIGATION OF DRAG REDUCTION FOR TRACTOR TRAILER VEHICLES WITH AIR DEFLECTOR AND BOATTAIL

Vincent U. Muirhead
University of Kansas Center for Research, Incorporated
Lawrence, Kansas

Prepared for
Dryden Flight Research Center
under Contract NSG 4021 and 4023

NASA
National Aeronautics and
Space Administration
Scientific and Technical
Information Office

1981

Intentionally Left Blank

TABLE OF CONTENTS

LIST OF SYMBOLS

A	Projected frontal area on a plane perpendicular to the centerline of the truck, scaled from A value from Reference 6
C_D	Coefficient of drag, D/qA
C_L	Coefficient of lift, L/qA
C_M	Coefficient of pitching moment, PM/qAc
C_Y	Coefficient of side force, SF/qA
C_ℓ	Coefficient of rolling moment, RM/qAc
C_N	Coefficient of yawing moment, YM/qAc
C_{D_X}	Coefficient of drag, configuration X
C_{P_b}	Coefficient of base pressure, $(P_b - P_A)/q$
c	Reference length (vehicle length for C_M) (vehicle width for C_ℓ, C_N)
D	Drag (truck axis)
D_e	Equivalent diameter, $\sqrt{4A/\pi}$
L	Lift (truck axis)
P	Power
P_A	Atmospheric pressure
P_b	Base pressure
PM	Pitching moment (truck axis)
q	True dynamic pressure in wind tunnel test section, $\frac{1}{2}\rho V^2$
RM	Rolling moment (truck axis)
R_N	Reynolds number (based on equivalent diameter), $\rho V D_e \mu$
SF	Side force (truck axis)
V	Relative wind speed = Wind tunnel airspeed

LIST OF SYMBOLS (cont'd)

V_1	Vehicle speed
V_2	Side wind component
W	True wind speed
YM	Yawing moment (truck axis)
β	Wind angle relative to vehicle path
ρ	Air density
μ	Air viscosity
ψ	Yaw angle = Relative wind angle

LIST OF FIGURES

Figure

LIST OF TABLES

ACKNOWLEDGMENTS

The advice and comments of Mr. Edwin Saltzman, Dryden Flight Research Center, are gratefully acknowledged. The wind tunnel testing and data reduction were conducted by the following students in the Department of Aerospace Engineering, University of Kansas:

Steven Ericson, Undergraduate student

Michael See, Undergraduate student

Thomas Davidson, Undergraduate student

Charles Svoboda, Undergraduate student

1.0 INTRODUCTION

A variety of add-on devices for tractor-trailer vehicles have been suggested to reduce the aerodynamic drag of these vehicles. There are wide ranging numbers available which represent the performance of such devices. The National Science Foundation has sponsored a summary publication of claimed reductions in drag and fuel consumption from various add-ons, Brunow, reference 1. Results and/or claimed results from manufacturers of add-on devices, testers and users are summarized as follows by Brunow:

Type	Drag Reduction	Fuel Consumption
Deflectors	7% - 24%	6% - 33%
Guide/Turning Vanes	2% - 25%	3% - 20%
Rounded Corners/Fairing	10% - 34%	4% - 37%
Gap-Fillers	19%	6% - 13%

The effect of side winds on these devices was ignored.

Montoya and Steers[2] conducted full-scale coast-down tests of five specific add-on devices for a cab-over-engine tractor-trailer combination. Device "A," a cab mounted air deflector, provided a 24% aerodynamic drag reduction with a 157.5 cm (62") gap between the tractor and trailer. A 16% drag reduction occurred with a 101.6 cm (40") gap. These values were obtained at zero wind conditions. Limited data indicated that the drag reduction was decreased by the presence of cross winds. Follow-on fuel consumption tests by Steers, Montoya and Saltzman[3] resulted in a fuel savings of 10% when using device "A" at the larger gap distance at 88.5 kilometers per hour (55 mph).

Full-scale coast-down tests were made by Sheridan and Grier[4] of four modifications of a 1966 Chevrolet, cab-behind-engine truck with a model 60 cab and box-shaped cargo compartment. Configuration "B," rounded forward edges of the cargo compartment, produced a 30% decrease in drag over configuration "A," the baseline unmodified vehicle. Configuration "C," "D" and "E," add-on flow vane concepts, decreased the drag from configuration "A" by 7% to 9%.

A substantial reduction in drag was achieved by streamlining a one-twenty-fifth scale model of a cab-over-engine tractor-trailer vehicle.[5] Configurations in common between this series of tests and full-scale tests by Steers and Saltzman[6] provided drag values which compare favorably.

The baseline model used in the tests of reference 5 has been restored to nearly its original condition to form a baseline for the present series of wind-tunnel tests. The present tests include an approximation of the best cab mounted device tested and reported in references 2 and 3, the cargo box mounted flow-vane concept reference 4, boattails as in reference 5, forced transition on the forward portion of the trailer and a reduced gap distance between the tractor cab and trailer. The results of these tests are reported herein and compared to some of the previous test results.

2.0 APPARTUS AND PROCEDURE

2.1 Models

The baseline version of the full-scale vehicle is shown in Figure 2.1.1 and its characteristics are contained in Table 1. Figure 2.1.2 shows the baseline wind tunnel model. The model was originally constructed for wind tunnel tests reported in Reference 5 from a commercially available one-twenty-fifth scale plastic model kit. However, in order to restore the previously tested model to the baseline configuration, much of the cab had to be rebuilt.

Subsequent configuration parts are shown in Figures 2.1.3, 2.1.4 and 2.1.5. The cab mounted deflector, Figure 2.1.3, is a one-twenty-fifth scale model approximation of device "A" as reported in Reference 2 and 3. The boattail, Figure 2.1.4, was constructed of balsa. The flow separation station on the boattail was determined at zero yaw by use of tufts. The boattail was cut at this station to provide the chopped-boattail configuration.

Two sets of flow-vanes, Reference 4, were constructed from brass as shown in Figure 2.1.5. The several configurations were assembled and tested according to Figure 2.1.6. Forced transition as indicated in Figure 2.1.6 was provided on the top and sides of the forward end of the trailer by the addition of a 1.27 cm (0.5") strip of fine 220 grit.

Two gap distances were used between the model tractor and trailer which were one-twenty-fifth scale values of the full scale gaps of references 2 and 3. The subscale gap distances were 6.29 cm (2.48") and 4.06 cm (1.60"). The decrease in gap was accomplished by the addition of a balsa block to the front of the trailer.

2.2 Mounting

The wind tunnel mounting system for the models, Figure 2.2.1, was the same system that had been used on previous tests[5]. The ground board enclosed the balance mounting strut and mounting plate. The model was held to the mounting plate by six adjustable rods attached to the tractor and trailer frames and running through the wheels. The model was adjusted vertically on the rods to position the model to the correct height above the ground board. The bottom of the wheels were sanded off so that they did not touch the ground board during the tests. The ground board contained three circular slots to allow the model to be rotated thirty degrees in each direction. During the tests the slots were covered except for a small clearance around each mounting rod.

The horizonal pressure gradient on the ground board was zero. The board was tufted to check for flow separation. The front of the ground board was rounded slightly to eliminate a small flow separation at the leading edge.

2.3 Tests

The tests were conducted in the University of Kansas, .91 by 1.29 meter wind tunnel at Reynolds numbers of 3.58×10^5 to 6.12×10^5 based upon the equivalent diameter of the vehicles or 18.64×10^5 to 32.00×10^5 based upon the length of the basic test model, Configuration 1. The Reynolds number was controlled by adjusting the wind tunnel airspeed from 164.2 to 289.8 kilometers per hour (102.0 to 180.1 mph). Tests were made at yaw (relative wind) angles of 0°, 5°, 10°, 20° and 30° on the configurations at four different Reynolds numbers. Force and moment data were obtained from a six component strain-gaged balance. Base pressures were measured by a pressure transducer. For Configurations 4, 5, 6, 10, 13, 16 and 17 the base pressure orifice was located at the boattail apex. For Configurations 1, 2, 3, 7, 8, 9, 14, 15, 18 and 19 the orifice was located at the center of the base region.

Wind tunnel test data were obtained through a newly installed analog/digital data system. The system was controlled by a Hewlett Packard 9825 calculator. Calibraton of the analog/digital system indicated an overall system error of less than ± 1% throughout the measuring range. This compared with the previous system error of ± 2% at full scale, increasing to ± 6% at 1/3 full scale and continued increasing error with decreasing scale.

The model and ground board were mounted and remounted a number of times to check repeatability. The mounting error for the combination of ground board and model was ± 2% except for lift and moments at small angles of yaw. These lift and drag measurements were very small and sensitive to small mounting errors. The data presented were obtained in three mountings: (1) Configurations 1, 2, 3, 4, 5, 6, 7, 8, 9, 10, 13, 14, 15, 16; (2) Configurations 11, 12; (3) Configurations 17, 18, 19.

3.0 RESULTS AND DISCUSSION

3.1 Drag

Drag coefficients were computed from the force acting along the model axis. The reference area used was the projected frontal area (A) for all configurations, including numbers 11 and 12 which did not include the trailer. These coefficients were plotted as a function of Reynolds number at each yaw angle on work plots, which are not included in this report. Subsequently drag coefficient values were extracted from these plots at a Reynolds number of 6×10^5 (based upon equivalent diameter). These values are shown in Table II. Figure 3.1.1 shows the variation of the drag coefficient with yaw (relative wind) angle at this Reynolds number for Configuration 1. It will be noted that the drag coefficients for Configuration 1 repeat those in Reference 5 within 4.4% or less, except for the 30° relative wind angle where the drag coefficient from the earlier tests is higher by 8.4%. Figures 3.1.2, 3.1.3, 3.1.4, 3.1.5 and 3.1.6 compare the drag coefficients of the nineteen configurations tested at various yaw angles for a Reynolds number of 6×10^5. These drag coefficients were normalized by dividing each drag coefficient by the drag coefficient for Configuration number 1 for those configurations without forced transition; and, for those coefficients having forced transition, the drag coefficient values from Configuration number 2 were used for normalization purposes, at each respective yaw angle.

Benefits and decrements resulting from the various modifications are given in percentage form in Table III. The drag coefficient increments are calculated relative to a baseline configuration, either configuration 1 or 2 depending on whether the boundary-layer transition was natural or forced, respectively. The percentage change in drag coefficient was then obtained by dividing the incremental drag coefficient by the appropriate baseline value, i.e. configuration 1 or 2.

Table IV uses a format similar to that of Table III, however, in this case incremental benefits are calculated for only two of the most promising modifications using several different configurations as a baseline reference. These incremental benefits are then divided (normalized) by the drag coefficients from configurations 1 or 2, whichever was appropriate with regard to the nature of the boundary-layer transition, as was done in Table III. The intent of Table IV is to provide a qualitative assessment of the consistency of the benefits provided by these two modifications in the presence of one or two other geometric differences which both the "test" configuration and the "baseline" vehicle have in common. Though there are variations in the drag increments from each of these two modifications, there is a characteristic level of drag reduction that is provided by each in spite of the other geometric differences imposed upon the respective "baseline" and "test" configurations compared in Table IV.

Table V shows comparisons of results from the present tests with results from configurations "in common" from references 2, 3 and 6.

The drag data shown in Tables II, III and IV and other data obtained during the tests indicate the following:

1. The effect of Reynolds number was small.
2. The transition strip on the forward end of the trailer produced a slight increase in drag (0.6%) at 0° wind angle and an average increase of 0.3% over a range of wind* angles from 0° to 20°.
3. Device "A" alone produced a decrease in drag of 19.9% at 0° wind angle and an average 5.4% decrease over a wind* range from 0° to 20°. In combination with other modifications Device "A" produced a decrease in drag from 18.8% to 24.9% at 0° wind angle. Over the 0° to 20° wind* angle range the corresponding average decrease ranged from 2.6% to 6.7%.
4. The boattail alone produced a decrease in drag of 5.4% at 0° wind angle and an average 6.3% decrease over a range of wind* angles from 0° to 20°. In combination with other modifications the boattail produced a decrease in drag of 3.0% to 6.1% at 0° wind angle. Over the 0° to 20° wind* angle range the corresponding average decrease ranged from 3.2% to 8.0%.
5. The small gap between the tractor and the trailer produced a decrease in drag of 6.3% at 0° wind angle and an average 8.1% decrease over the 0° to 20° wind* angle range.

*relative wind angle, ψ

6. Over the operating range of wind* angles of 0° to 20° Configuration 17 (Device "A" with small tractor-trailer gap and boattail) provided the largest drag reduction.
7. A comparison of the drag results for the small or large radius flow-vane indicate that these devices were not very helpful in reducing drag. Though such a device produced a significant reduction in drag on a standard 2-axle truck, Reference 4, it is apparent that the cab geometry and the gap distance involved in the present cab-over-engine tractor and trailer applications will not allow the flow-vane to perform effectively.

The base pressure data variation with relative wind angle is shown in Figure 3.1.7 for Configuration 1. The data, obtained for every two degrees of relative wind, were rechecked for all configurations because there are some disagreements with the data of Reference 5. It is believed that the tests of Reference 5 were in error in some cases because of pinching of the pressure tube leading from the model. Table VI contains the base pressure data for all configurations except 11 and 12 (cab without trailer). Figures 3.1.8, 3.1.9, 3.1.10 and 3.1.11 provide a comparison of the base pressure coefficients. For every configuration having the boattail or chopped boattail, the center body or apex base pressure coefficients are significantly less negative than the blunt based configurations, especially for relative wind angles below 20°.

The power required to overcome the aerodynamic drag for a full-scale vehicle, Configurations 1 and 2, at 88.5 kilometers per hour (55 mph) ground speed was calculated using the wind speeds of 0, 15.3 and 30.6 kilometers per hour (0, 9.5 and 19.0 mph). Wind angles of 0° through 180° relative to the vehicle path were used, Figure 3.1.12. The corresponding values for Configurations 3, 4, 5, 17 and 19 are given in Figures 3.1.13 through 3.1.17. Table VII provides the power required to overcome aerodynamic drag for all configurations. These data represent: (1) the no-wind condition, (2) a 15.3 km per hour (9.5 mph) wind and (3) a 30.6 km per hour (19.0 mph) wind, each averaged over the entire range of directions, from 0° to 180°.

The calculated values of average power required to overcome aerodynamic drag have special significance for the lower of the two wind speeds i.e., 15.3 km per hour (9.5 mph). This is because this wind speed closely approximates the average annual winds for the 48 contiguous United States. Thus fuel consumption values calculated from this wind speed will include the approximate wind effects over an extended period of time, like a year or more.

Table VIII contains the values of average fuel consumption per hour to overcome the aerodynamic drag and the resulting fuel costs in the presence of the aforementioned average annual winds. The cab mounted air deflector, boattail and the small gap produced calculated fuel savings of 5%, 8%, and 5% (respectively) of the aerodynamic portion of the fuel budget. Actual experience with cab mounted devices often provide greater savings, which suggests that the approach used herein to account for wind effects may be too conservative.

3.2 Side Force

The side force coefficients were computed from the forces acting on the wind tunnel model perpendicular to the model axis. The reference area used was the projected frontal area (A). The variation of side force with yaw for Configuration 1 is shown in Figure 3.2.1 for a Reynolds number of 6×10^5. These data repeat those of Reference 5 within 3.8% or less. The side force coefficients for a Reynolds number of 6×10^5, corrected for wind tunnel flow angularity error, are contained in Table IX. A comparison of the side force coefficients of the various tractor trailer configurations is contained in Figures 3.2.2, 3.2.3, 3.2.4 and 3.2.5. Configurations including device A, flow-vanes or the small gap produced side force coefficients higher than the baseline, for yaw angles near 5 degrees, except when the boattail was also included. The boattail tended to reduce the sideforce coefficient, for $\psi = 5°$, regardless of the accompanying modifications.

3.3 Lift

The variation of the lift coefficient with yaw angle is shown in Figure 3.3.1. The reference area used was the projected frontal area (A). The lift coefficients of all configurations ($R_N = 6 \times 10^5$) are given in Table X. The lift forces were small and, therefore, very sensitive to mounting and measurement errors. Thus, at low yaw angles the percentage differences relative to the results of Reference 5 are large.

3.4 Pitching Moment

The pitching moment coefficients of Configuration 1 about a lateral axis 27.9 cm (11.0") from the front of the vehicle and 5.7 cm (2.25") above the ground plane are shown in Figure 3.4.1. The reference area used was the projected frontal area (A); the reference length (c) was the vehicle length. The pitching moment coefficients of all configurations are given in Table XI

($R_N = 6 \times 10^5$). These data for Configuration 1 differ significantly from the values in Reference 5. Repetition of the tests and careful checking of the data have established that the pitching moment data of reference 5 contained computational error.

3.5 Rolling Moment

The rolling moment coefficients of Configuration 1 about a central longitudinal axis 5.7 cm (2.25") above the ground plane are shown in Figure 3.5.1. The reference area was the projected area (A); the reference length (c) was the vehicle width. The rolling moment coefficients for all configurations corrected for flow angularity error are given in Table XII ($R_N = 6 \times 10^5$). These data for Configuration 1 differ from the values in Reference 5 which contained a computational error in the rolling moment data. Both rolling and pitching moment coefficients for all configurations of reference 5 contain the same computational error.

3.6 Yawing Moment

The yawing moment coefficient for Configuration 1 about a central vertical axis 27.9 cm (11.0") from the front of the vehicle are shown in Figure 3.6.1. The reference area used was the projected frontal area (A); the reference length (c) was the vehicle width. The yawing moment coefficients for all of the configurations corrected for flow angularity error are given in Table XIII ($R_N = 6 \times 10^5$). The values for Configuration 1 compare closely with those in Reference 5.

4. CONCLUSIONS

The cab mounted air deflector produced a calculated reduction in fuel consumption of about 5% of the aerodynamic portion of the fuel budget for a wind speed of 15.3 km/hr (9.5 mph) over a 0^o to 180^o wind angle range with a vehicle speed of 88.6 km/hr (55 mph).

The boattail produced a calculated reduction in fuel consumption of 7% to 8% under similar conditions. The decrease in gap distance produced a corresponding 5% reduction in calculated fuel consumption.

The effectiveness of a given add-on device was found to be very dependent on geometry (or flow conditions) of the original vehicle. Consequently the flow-vane concept, which produced significant improvements on a standard two-axle truck, provided no significant benefits when applied to a scale model of the tractor-trailer type of vehicle.

5. REFERENCES

1. Bronow, C. L., "An Evaulation of Truck Aerodynamic Drag Reduction Devices and Tests," Innocept, Inc., Dallas, Texas, June 1975.
2. Montoya, L. C. and Steers, L. L., "Aerodynamic Drag Reduction Tests on a Full-Scale Tractor Trailer Combinaton with Several Add-On Devices," NASA TM X-56028, December 1974.
3. Steers, L. L., Montoya, L. C., and Saltzman, E. J., "Aerodynamic Drag Reduction Tests on a Full-Scale Tractor-Trailer Combination and Representative Box-Shaped Ground Vehicle," Society of Automotive Engineers, Paper SAE 750703, August 1975.
4. Sheridan, A. E. and Grier, S. J., "Drag Reduction Obtained by Modifying a Standard Truck," NASA TM 72846, February 1978.
5. Muirhead, V. U., "An Investigation of Drag Reduction for Tractor Trailer Vehicles," NASA CR 144877, October 1978.
6. Steers, L. L. and Saltzman, E. J., "Reduced Truck Fuel Consumption through Aerodynamic Design," Journal of Energy, Vol. 1, No. 5, September-October 1977.

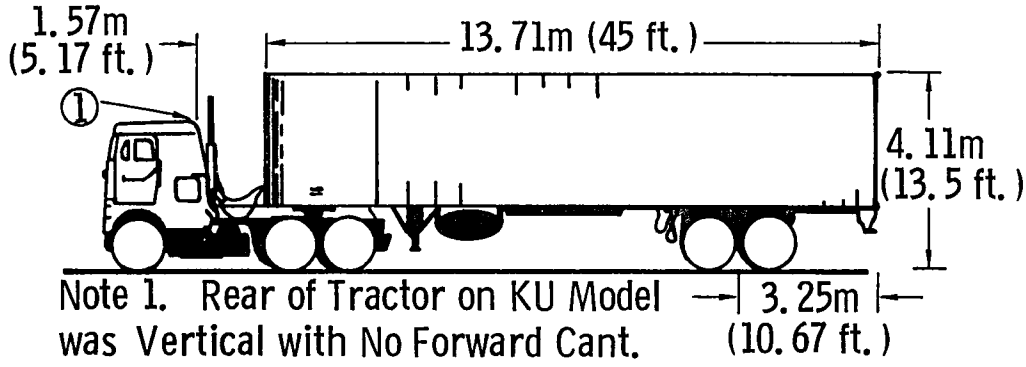

(a) Side View

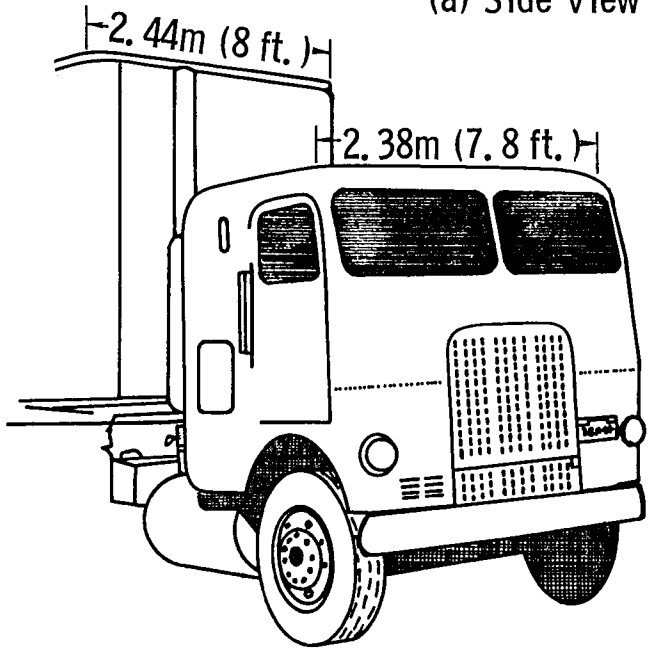

(b) Three-Quarter Front View

Figure 2.1.1 Full-scale Basic Vehicle (References 2, 3, 5 and 6)

Figure 2.1.2 Photograph of Baseline Wind Tunnel Model

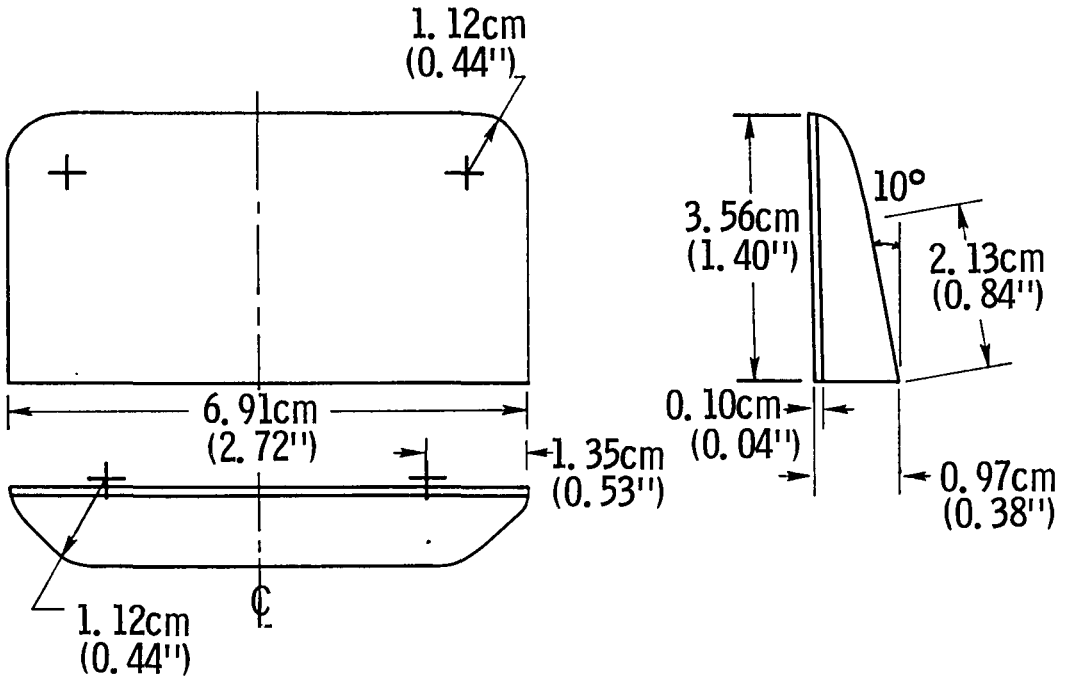

Figure 2.1.3 Air Deflector, approximation of Device "A" of Reference 2 and 3

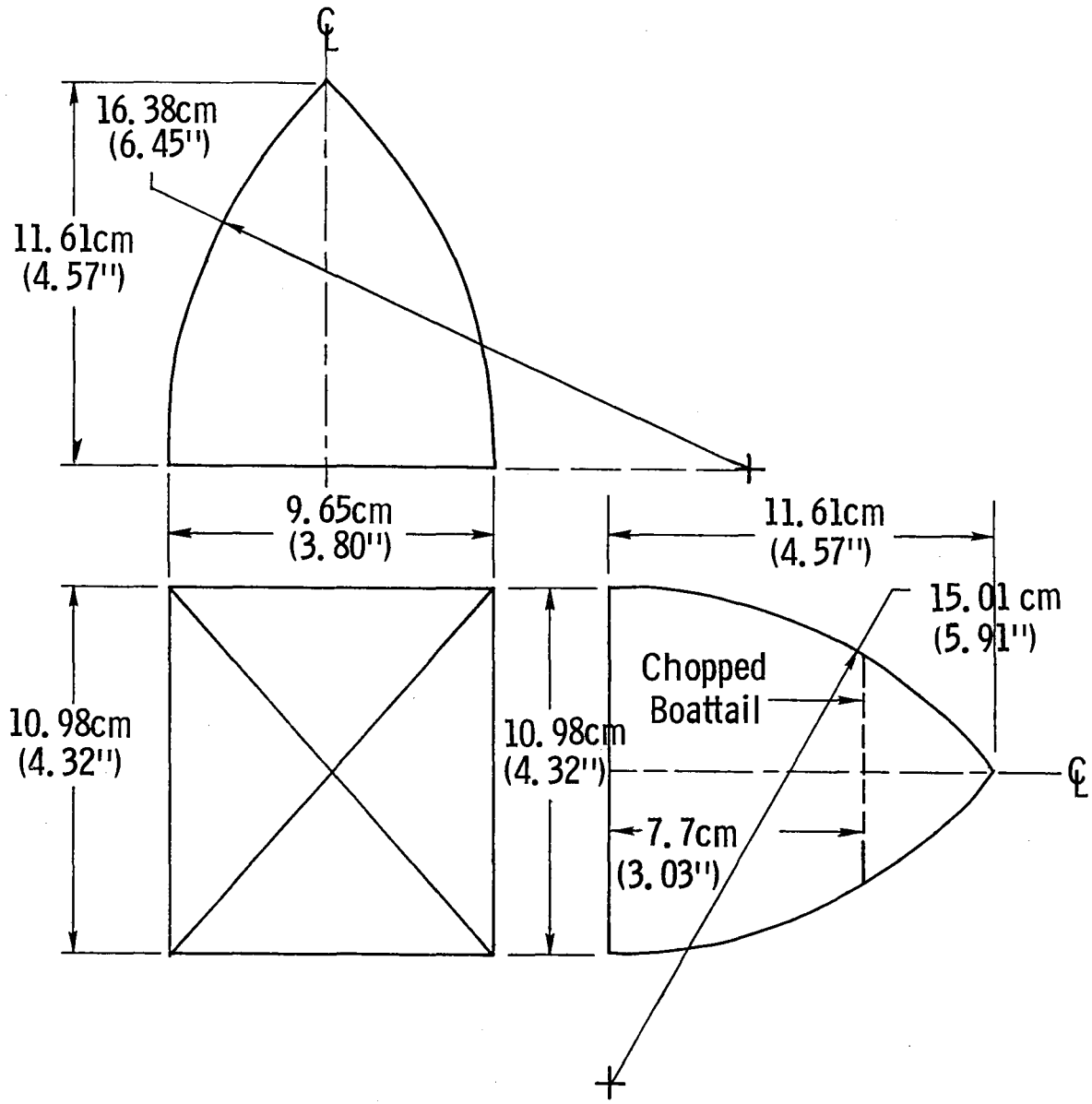

Figure 2.1.4 Boattail

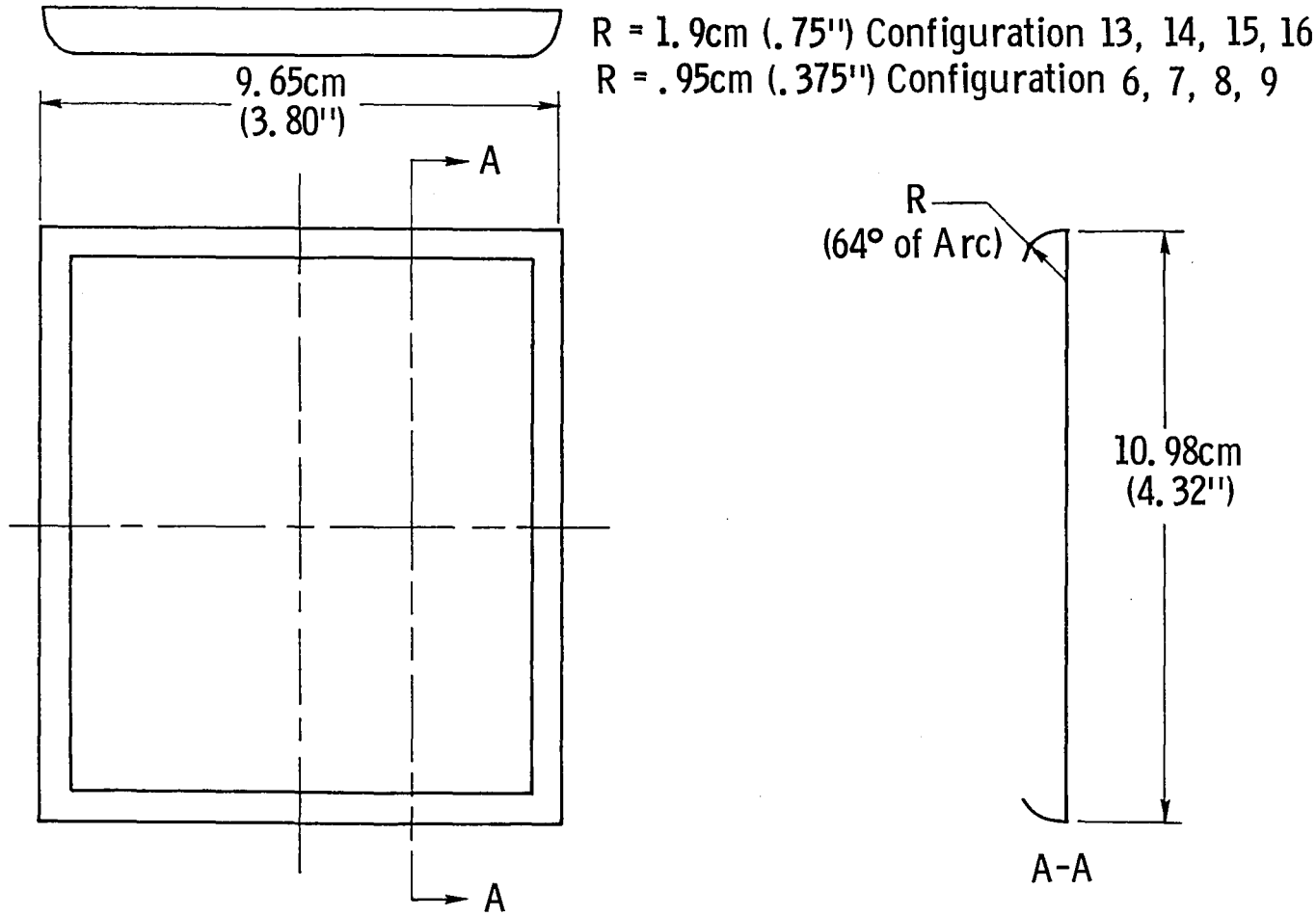

Figure 2.1.5 Flow-vane Concept (NASA TM 72846., Reference 4)

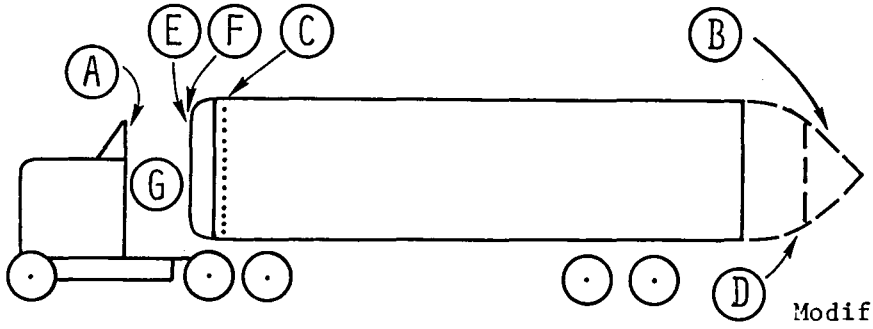

Modifications

No. #	Cab	Trailer	Forced Transition	Forebody	Rear
1	Y	Y	None	None	None
2	Y	Y	Y,C	None	None
3	Y	Y	None	A	None
4	Y	Y	None	None	B
5	Y	Y	None	A	B
6	Y	Y	Y,C	E	B
7	Y	Y	Y,C	E	D
8	Y	Y	Y,C	E	None
9	Y	Y	Y,C	A + E	None
10	Y	Y	Y,C	None	B
11	Y	None	None	None	--
12	Y	None	None	A	--
13	Y	Y	Y,C	F	B
14	Y	Y	Y,C	F	None
15	Y	Y	Y,C	A + F	None
16	Y	Y	Y,C	A + F	B
17	Y	Y	Y,C	A + G	B
18	Y	Y	Y,C	A + G	None
19	Y	Y	Y,C	G	None

Note: Y = Yes

A = Approximation of Device "A" as Reported in NASA TMX-56028

B = Full Boattail

C = Forced Transition, Top and Sides of Trailer - 1.27 cm (0.5" strip of 220 grit

D = "Chopped" Boattail, Location of Cut-off Determined by Tufting, other Flow Visual and Full-scale Van Data

E = Small Flow Vane, Concept as Described in NASA TM 72846 by Sheridan and Grier (Horizontal and Vertical Edges): Radius .95 cm (.375")

F = Large Flow Vane, Same Concept as E except Radius 1.9 cm (.75")

G = Gap Between Tractor and Trailer Reduced from 6.29 cm (2.48") to 4.06 cm (1.60")

Figure 2.1.6. Model Configuration Chart

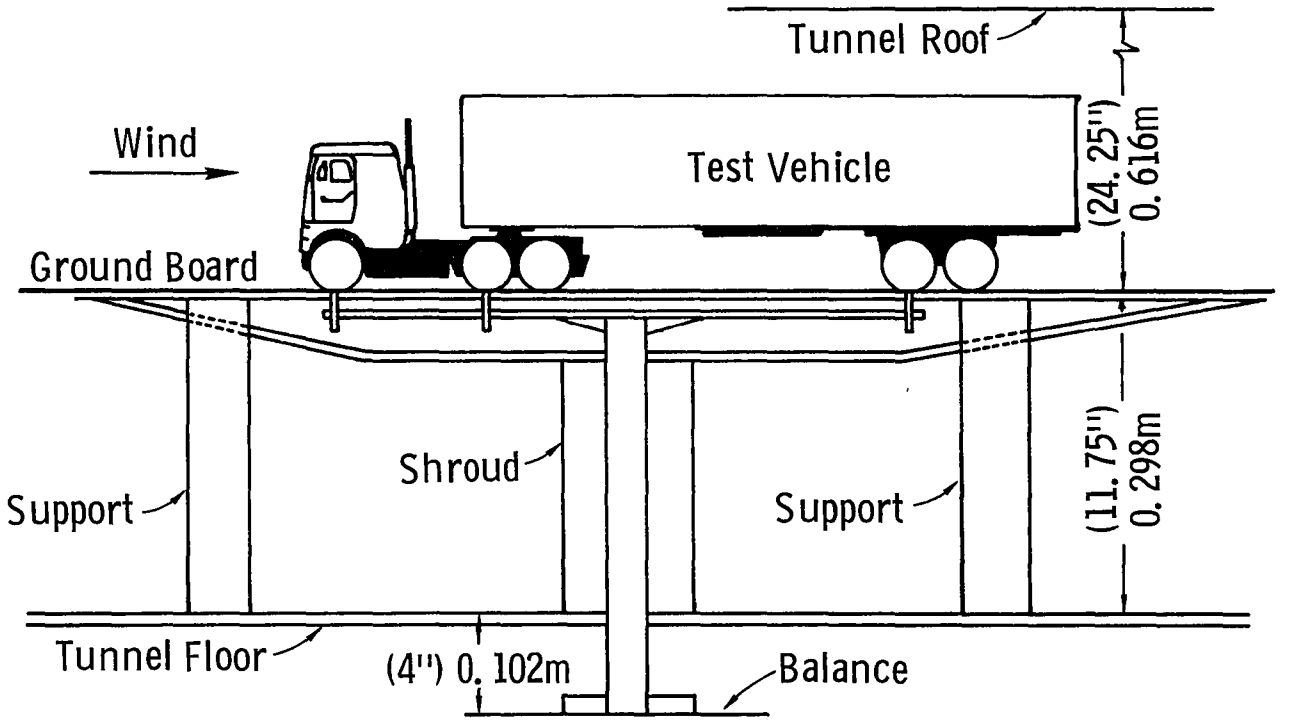

Figure 2.2.1 Wind Tunnel Mount

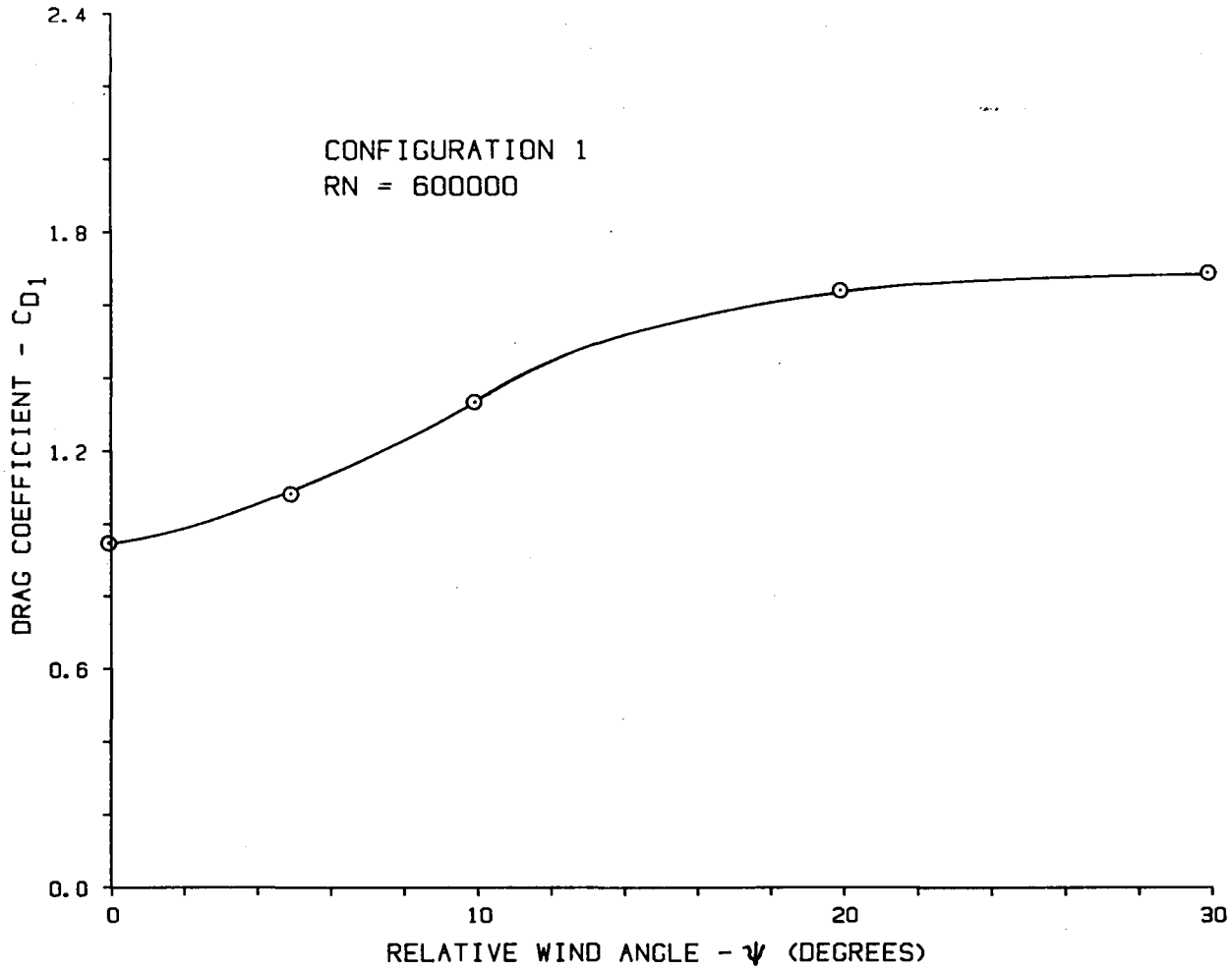

FIGURE 3.1.1 EFFECT OF RELATIVE WIND ANGLE ON DRAG COEFFICIENT C_{D_1}

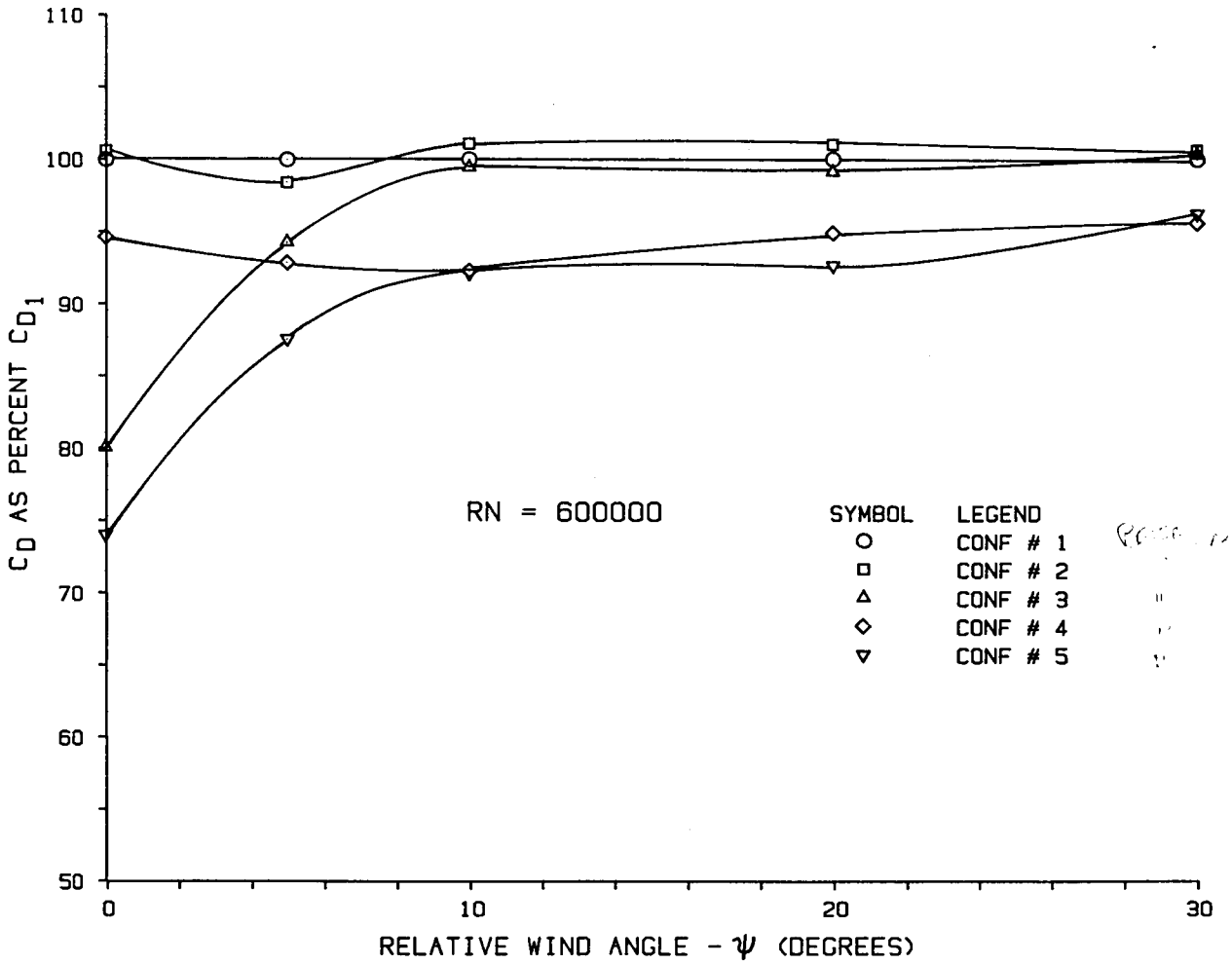

FIGURE 3.1.2 COMPARISON OF DRAG COEFFICIENTS, CONFIGURATIONS 1, 2, 3, 4, 5

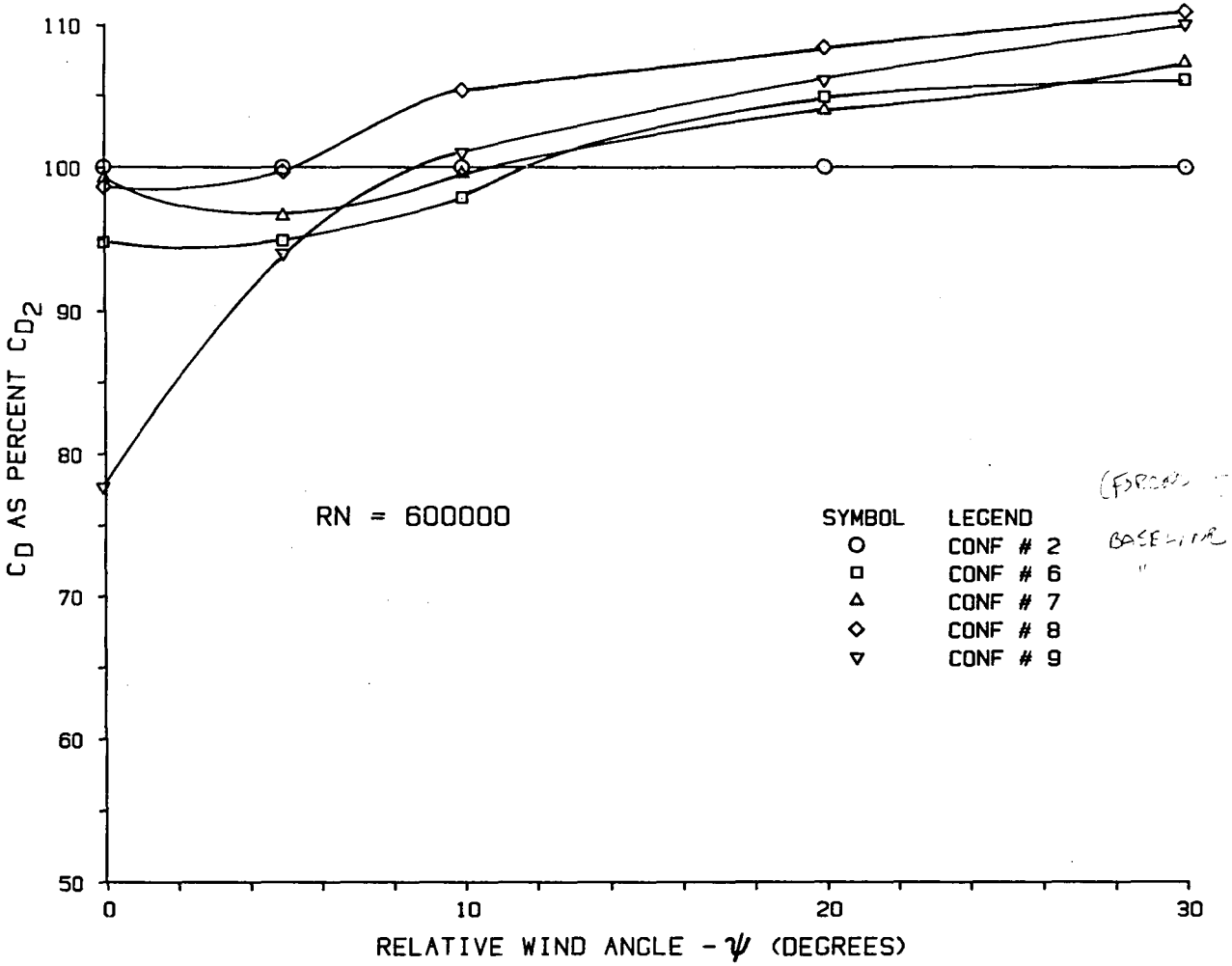

FIGURE 3.1.3 COMPARISON OF DRAG COEFFICIENTS, CONFIGURATIONS 2, 6, 7, 8, 9

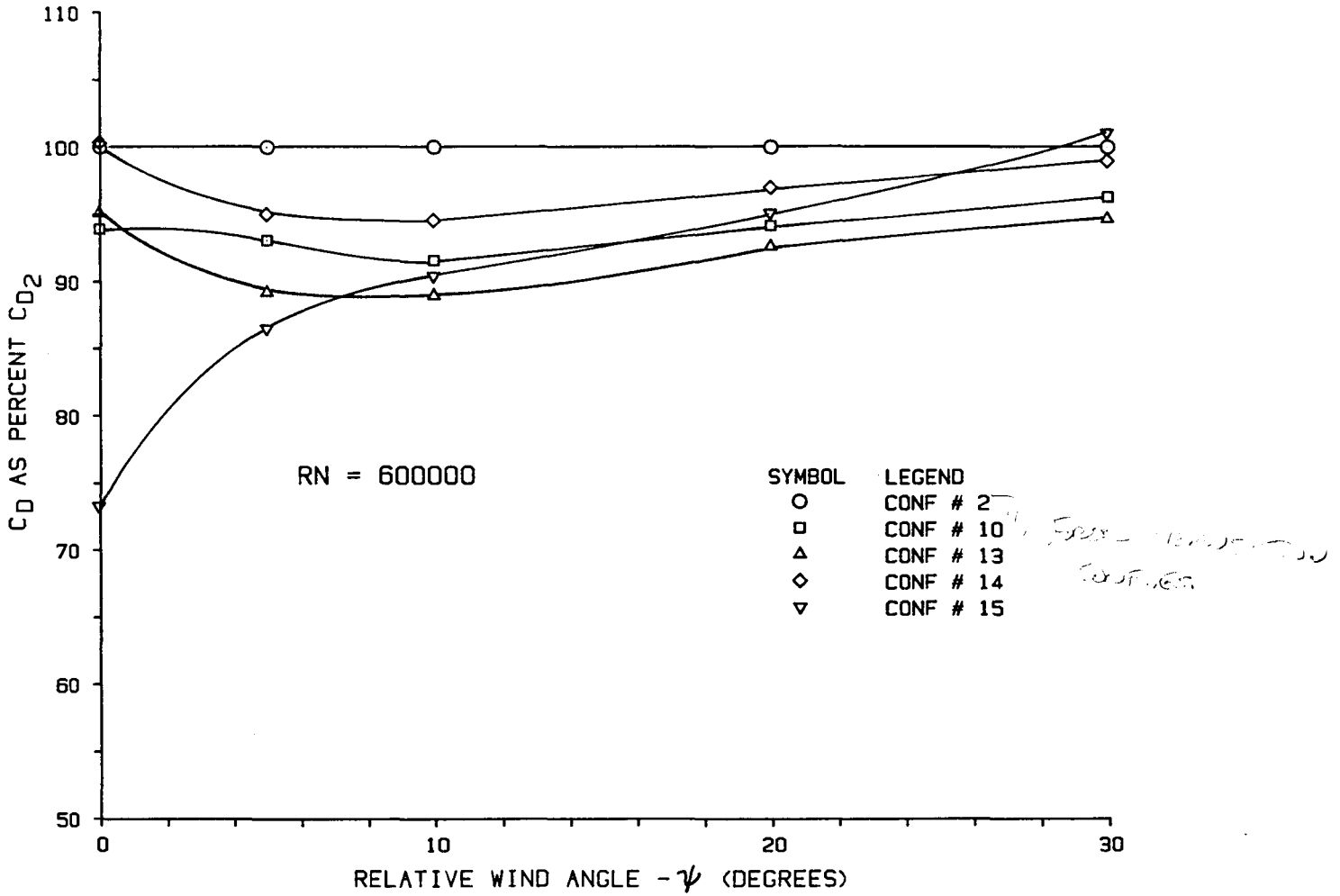

FIGURE 3.1.4 COMPARISON OF DRAG COEFFICIENTS, CONFIGURATIONS 2, 10, 13, 14, 15

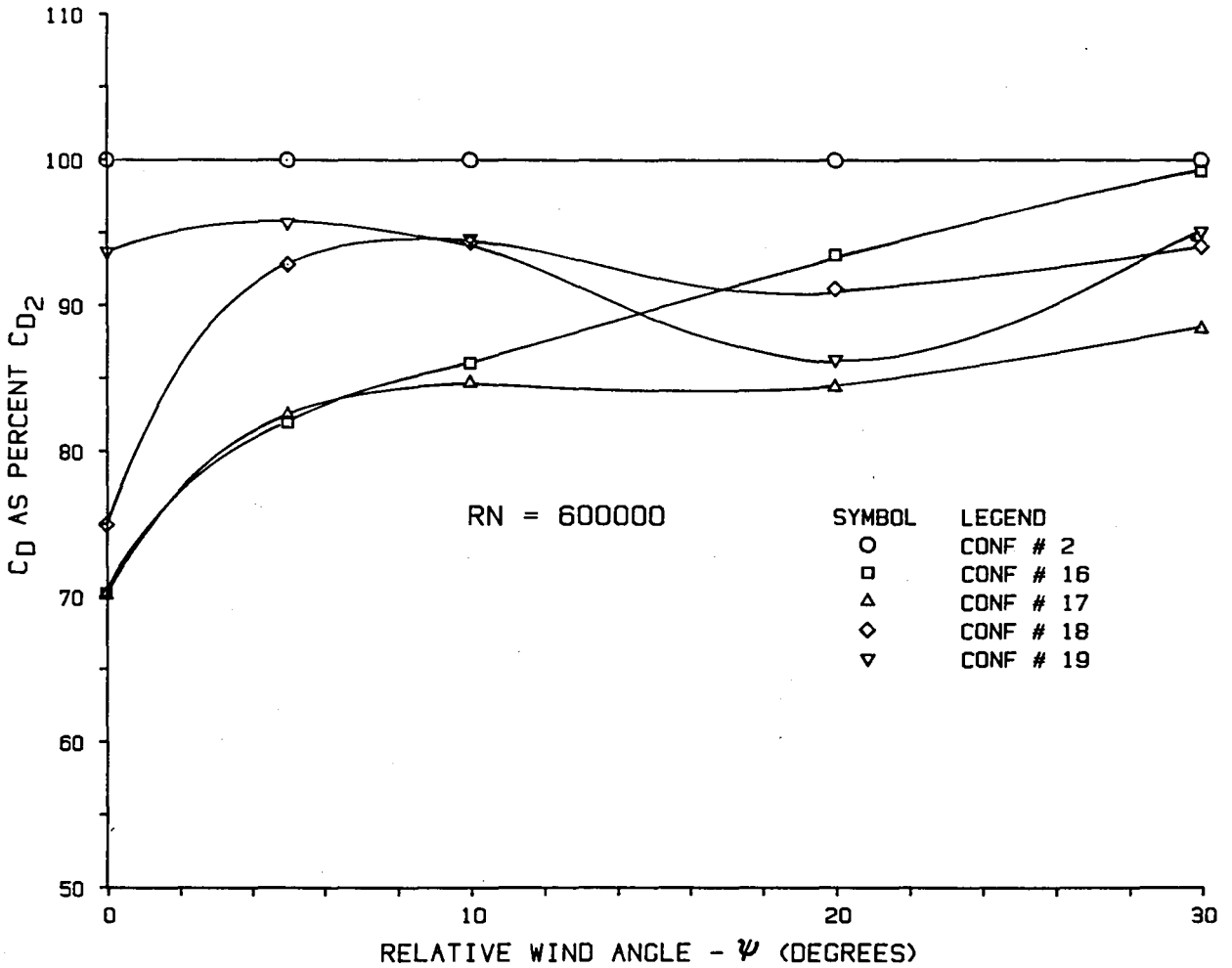

FIGURE 3.1.5 COMPARISON OF DRAG COEFFICIENTS, CONFIGURATIONS 2, 16, 17, 18, 19

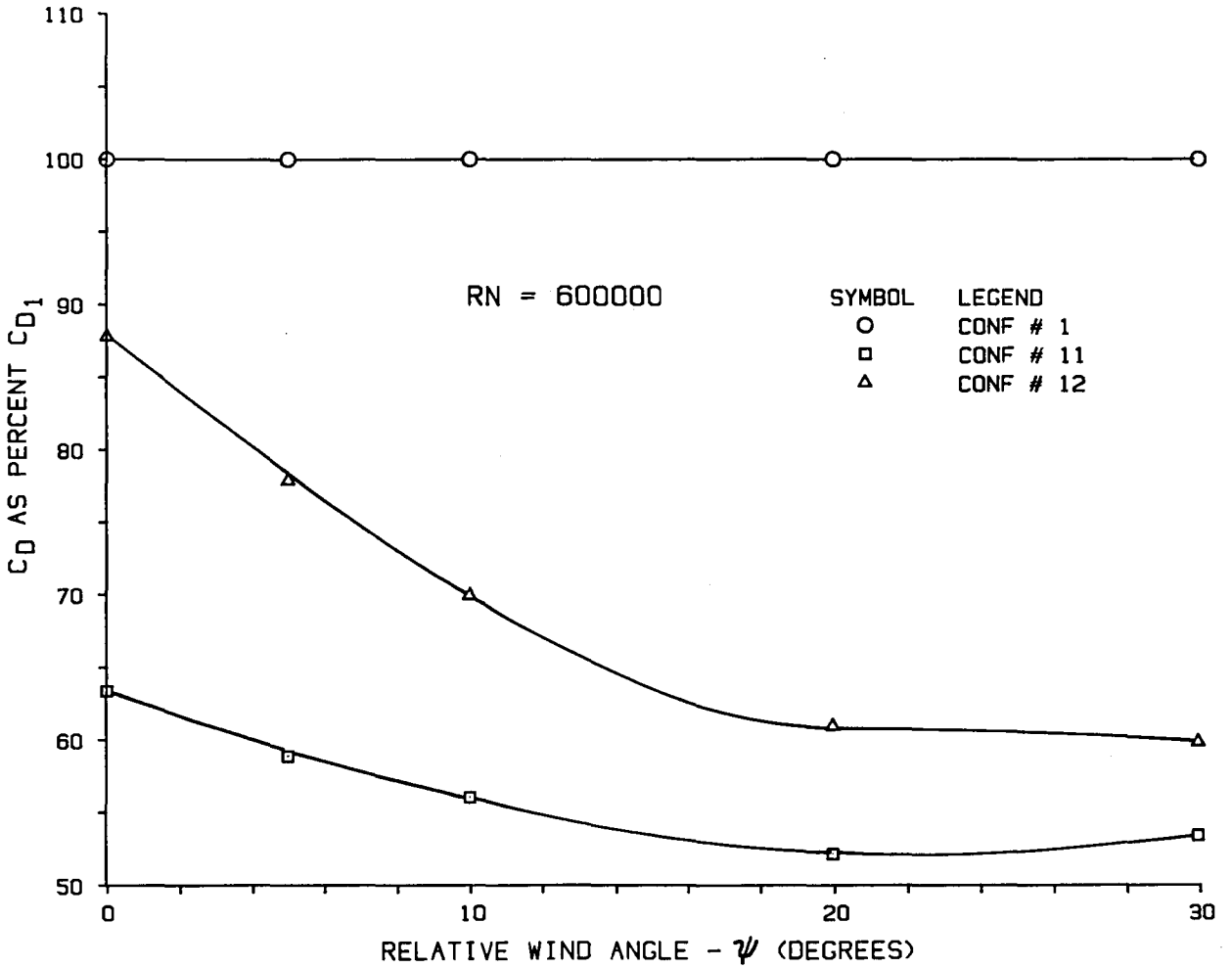

FIGURE 3.1.6 COMPARISON OF DRAG COEFFICIENTS, CONFIGURATIONS 1, 11, 12

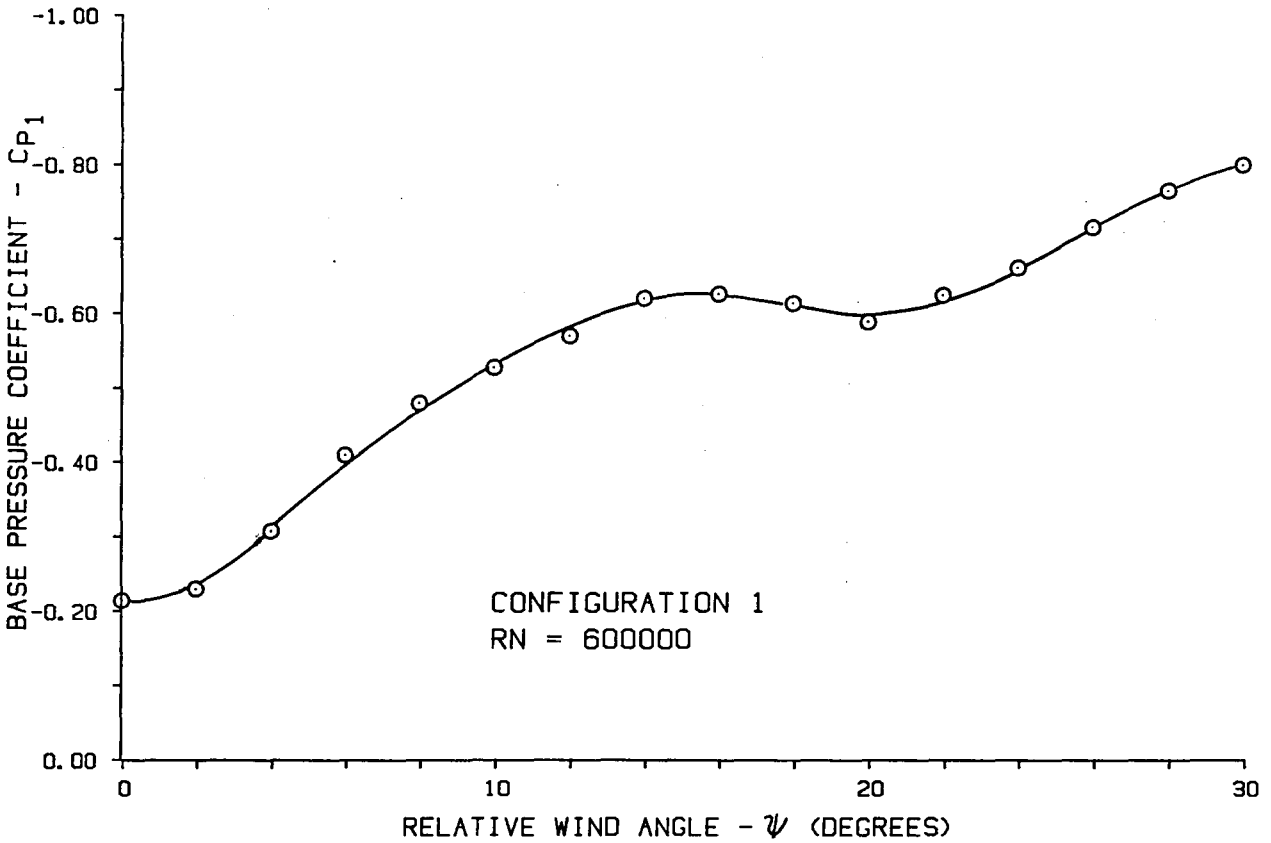

FIGURE 3.1.7 EFFECT OF RELATIVE WIND ANGLE ON BASE PRESSURE COEFFICIENT C_{P_1}

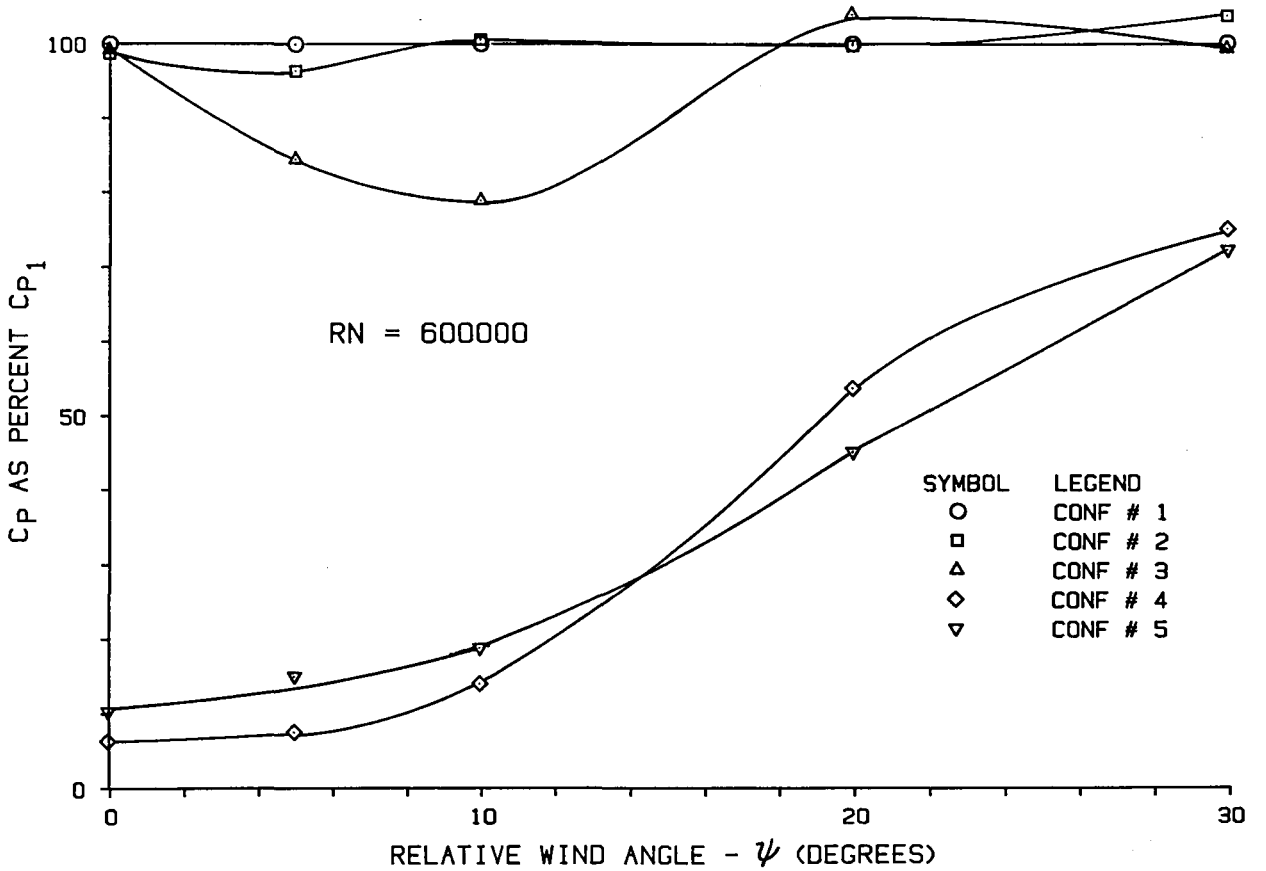

FIGURE 3.1.8 COMPARISON OF BASE PRESSURE COEFFICIENTS, CONFIGURATIONS 1, 2, 3, 4, 5

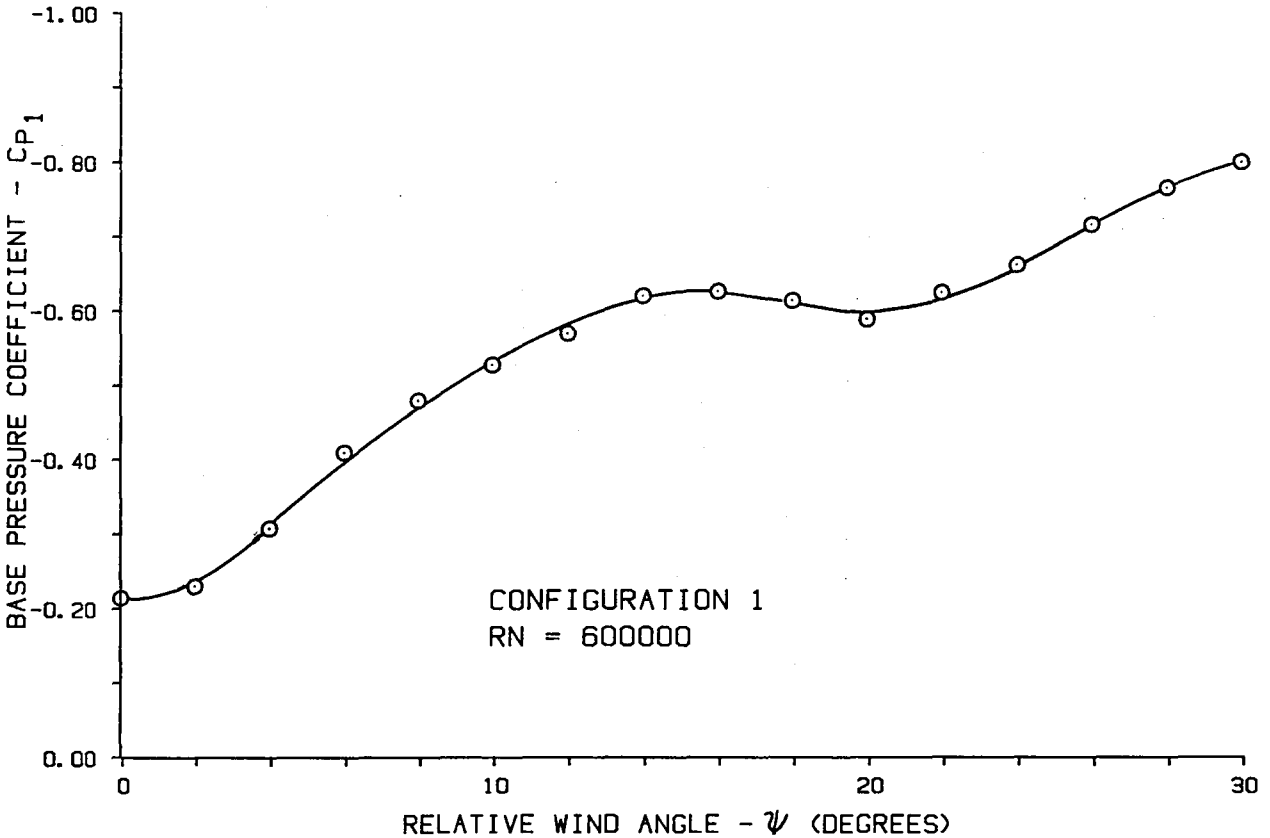

FIGURE 3.1.7 EFFECT OF RELATIVE WIND ANGLE ON BASE PRESSURE COEFFICIENT C_{P_1}

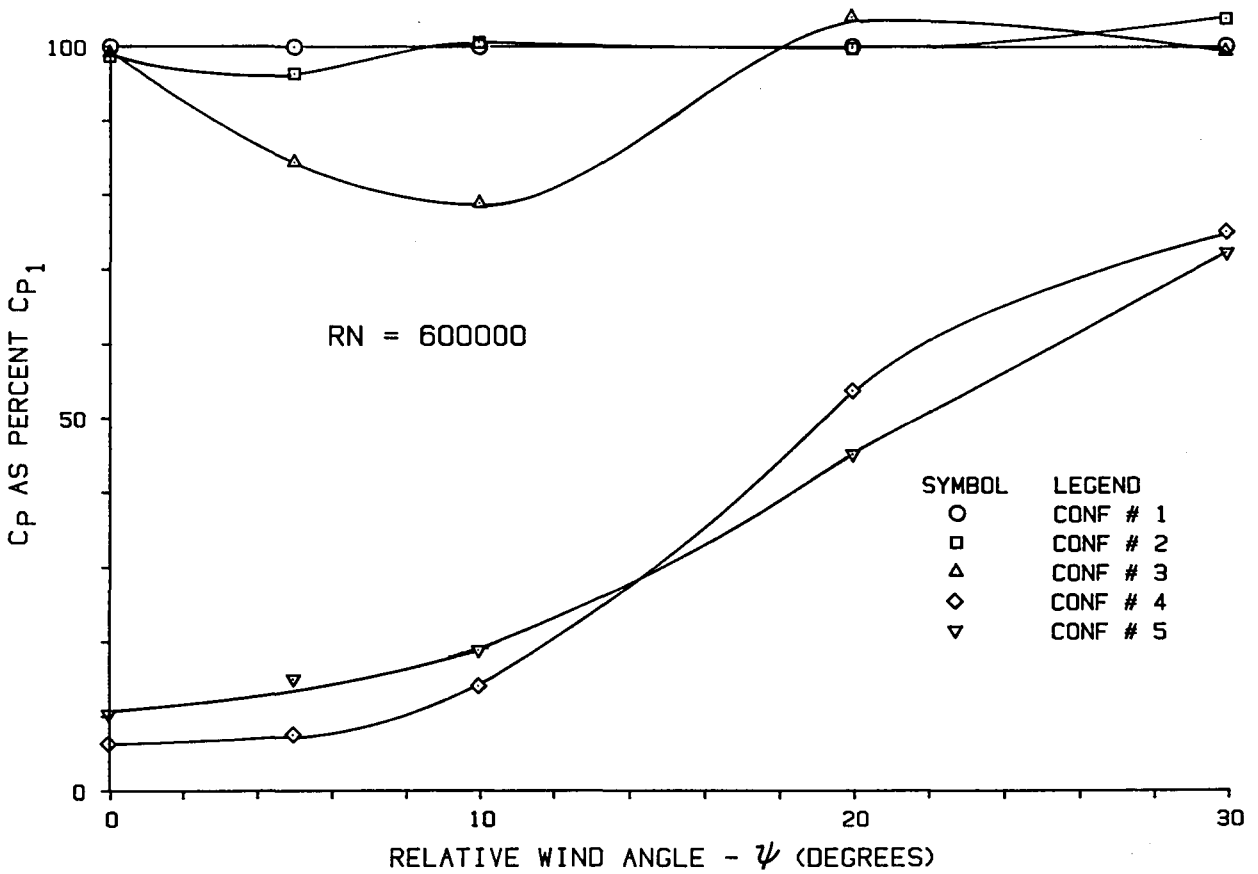

FIGURE 3.1.8 COMPARISON OF BASE PRESSURE COEFFICIENTS, CONFIGURATIONS 1, 2, 3, 4, 5

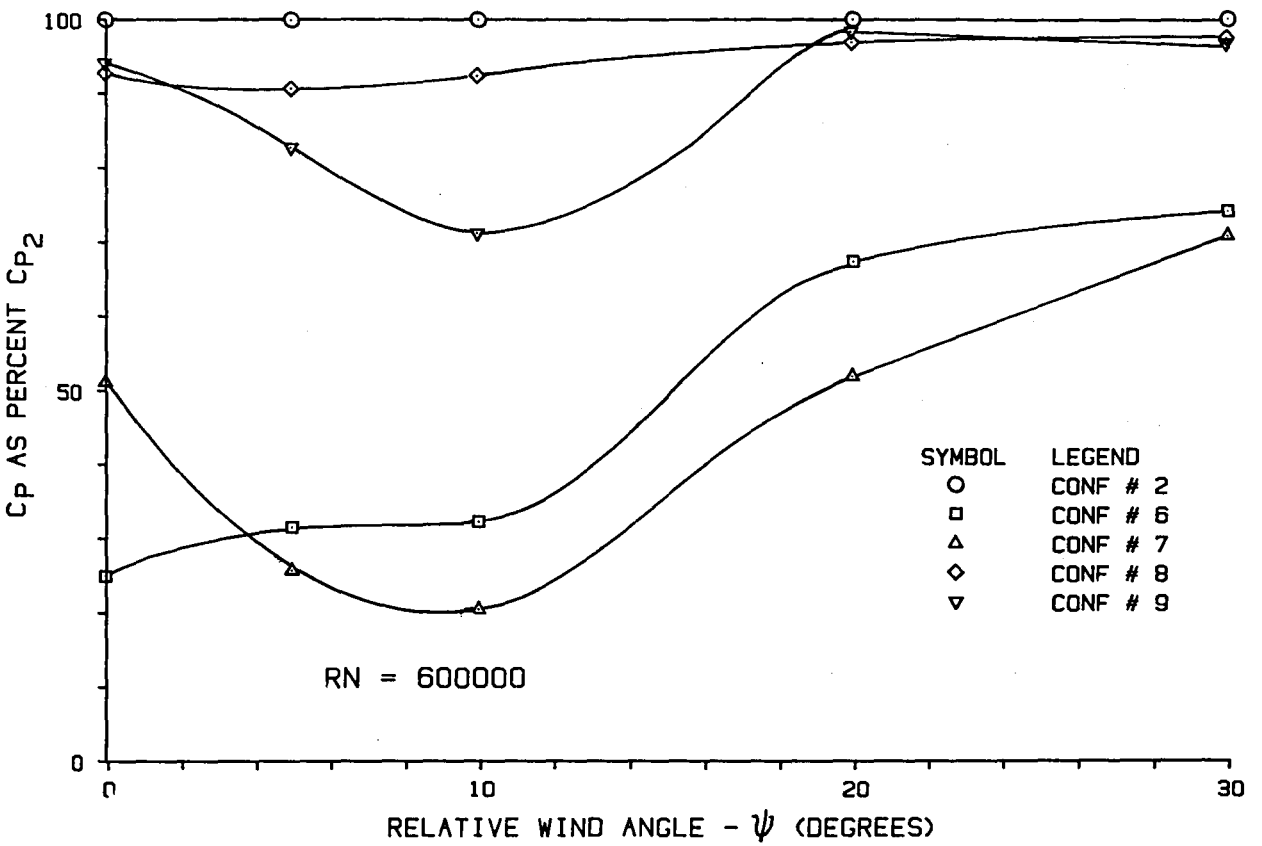

FIGURE 3.1.9 COMPARISON OF BASE PRESSURE COEFFICIENTS, CONFIGURATIONS 2, 6, 7, 8, 9

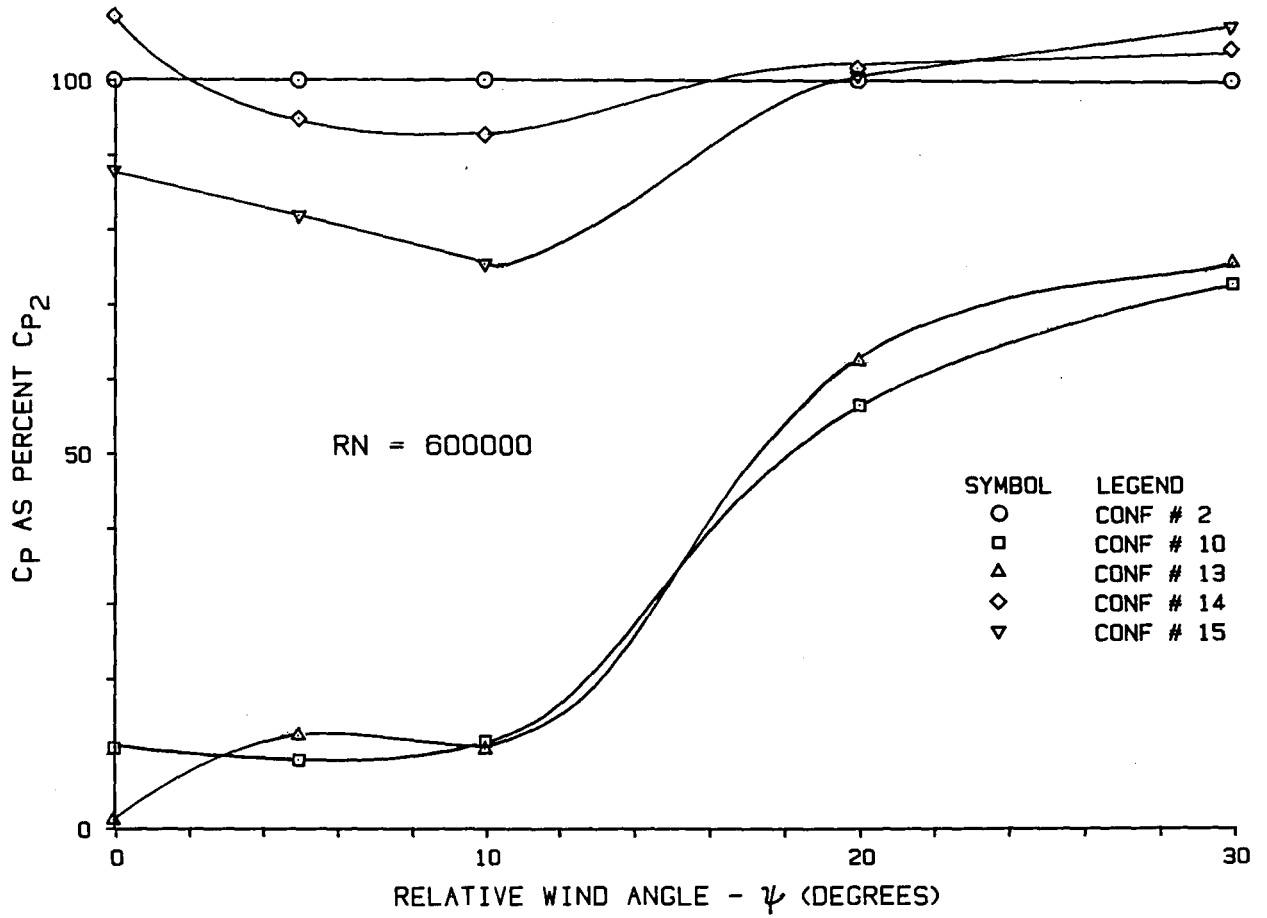

FIGURE 3.1.10 COMPARISON OF BASE PRESSURE COEFFICIENTS, CONFIGURATIONS 2, 10, 13, 14, 15

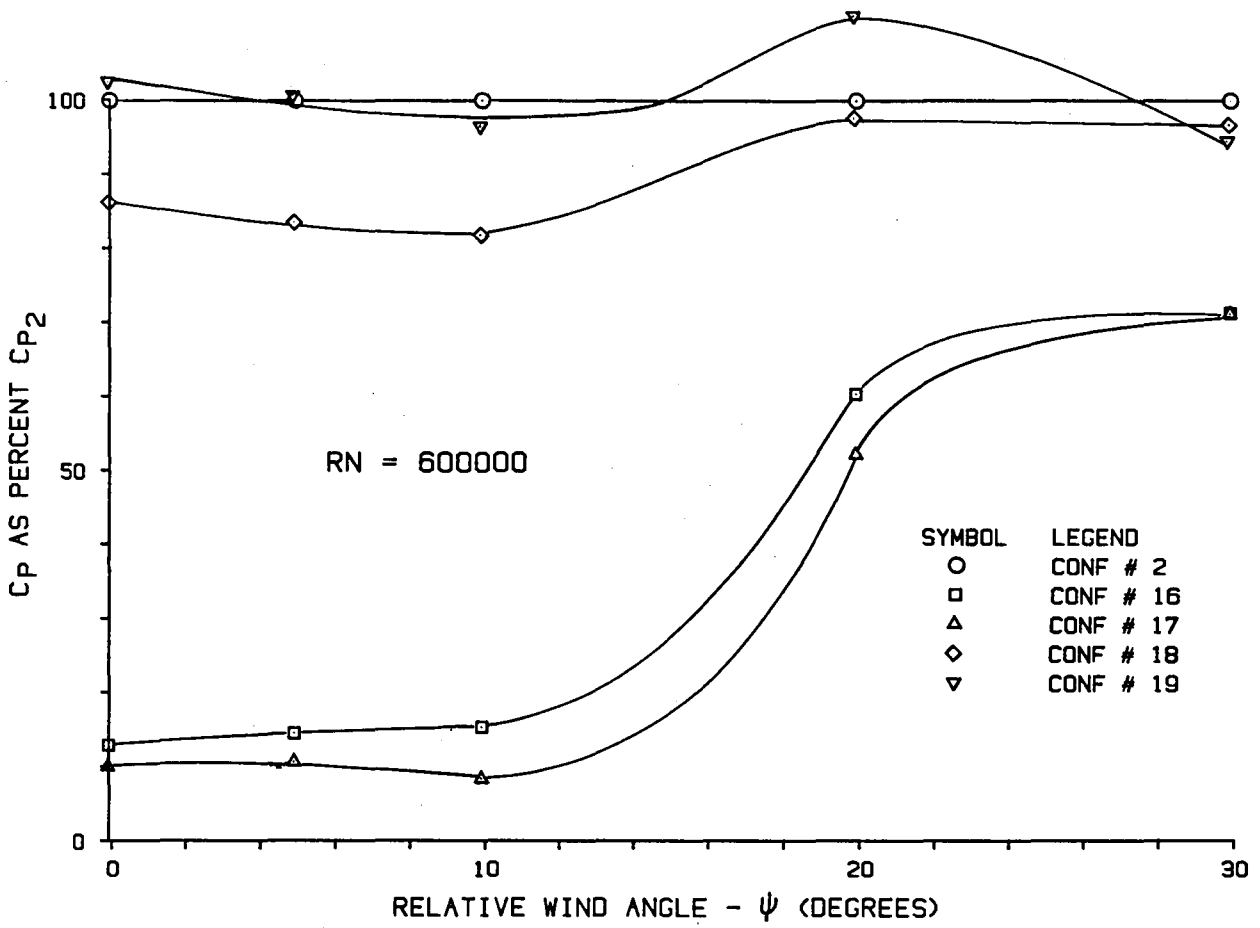

FIGURE 3.1.11 COMPARISON OF BASE PRESSURE COEFFICIENTS, CONFIGURATIONS 2, 16, 17, 18, 19

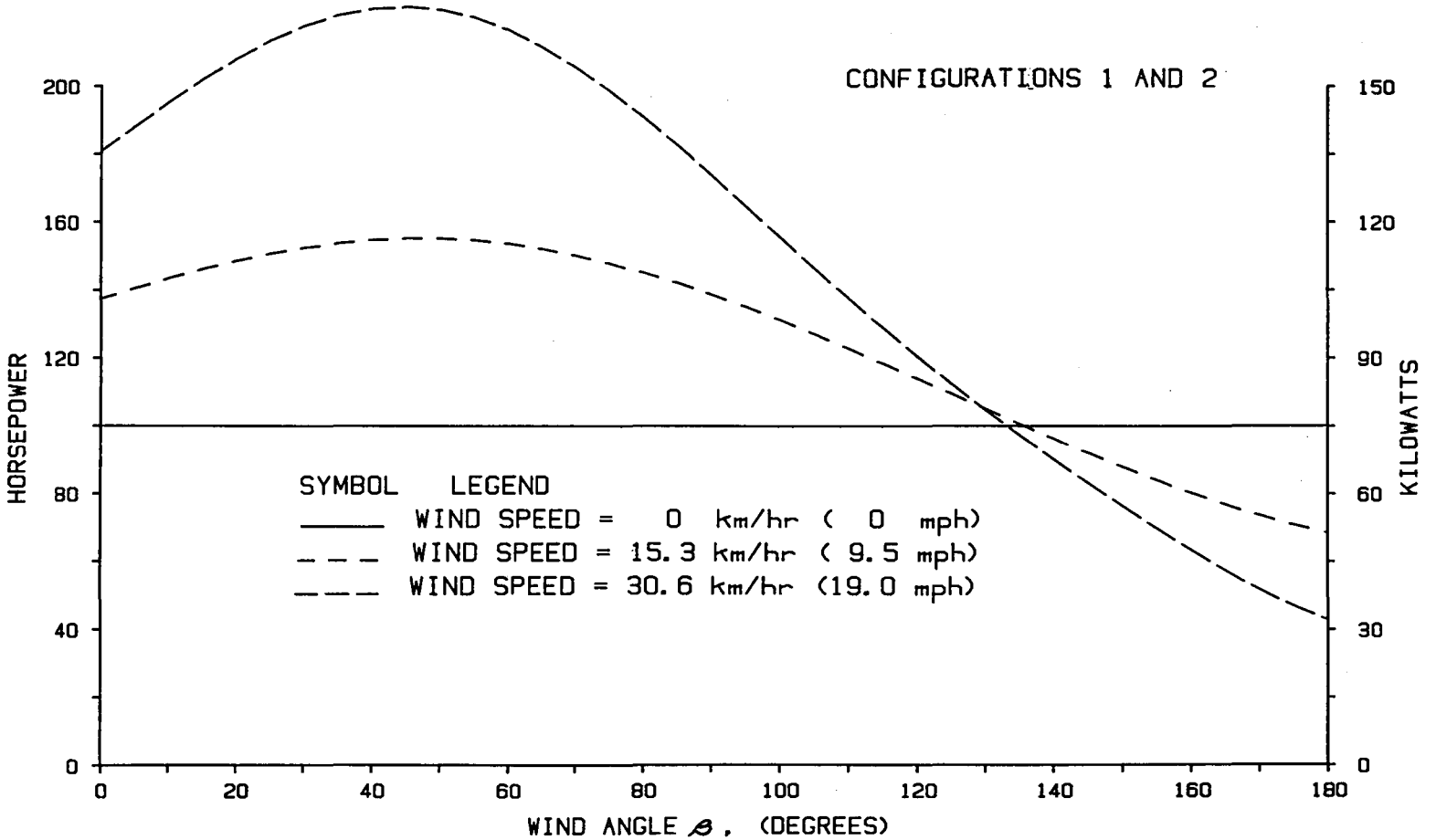

FIGURE 3.1.12 POWER REQUIRED TO OVERCOME AERODYNAMIC DRAG, CONFIGURATIONS 1 AND 2

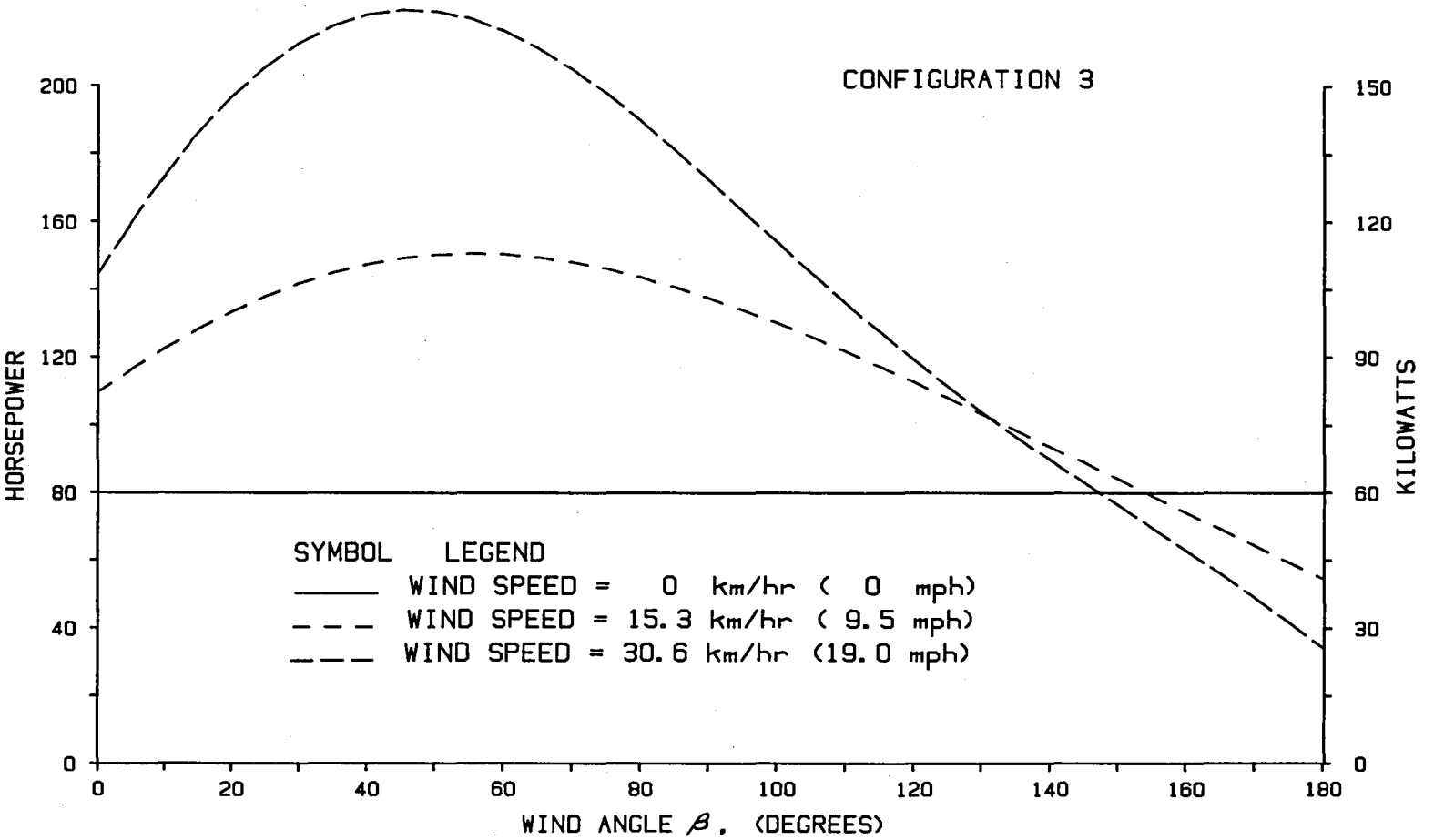

FIGURE 3.1.13 POWER REQUIRED TO OVERCOME AERODYNAMIC DRAG, CONFIGURATION 3

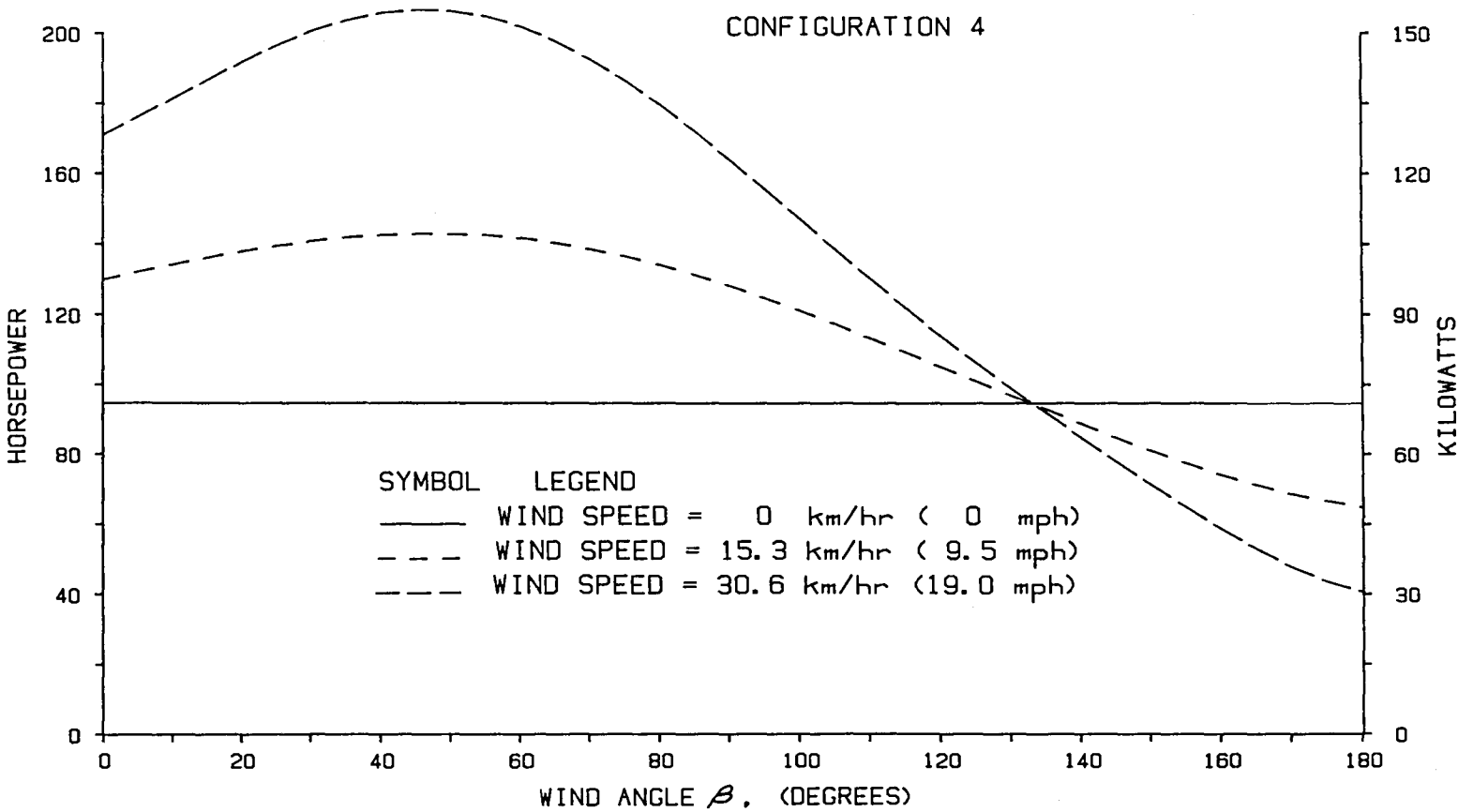

FIGURE 3.1.14 POWER REQUIRED TO OVERCOME AERODYNAMIC DRAG, CONFIGURATION 4

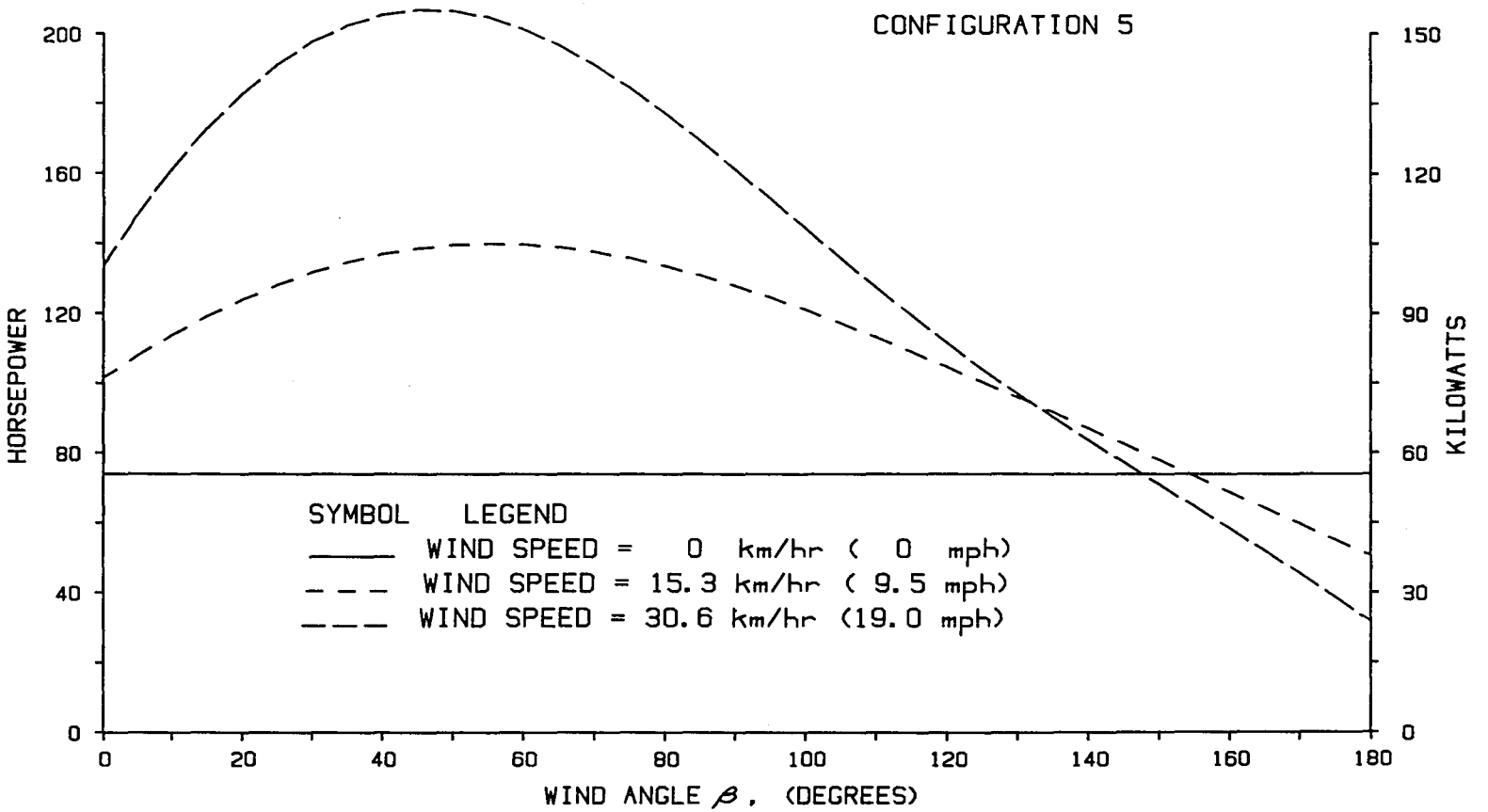

FIGURE 3.1.15 POWER REQUIRED TO OVERCOME AERODYNAMIC DRAG, CONFIGURATION 5

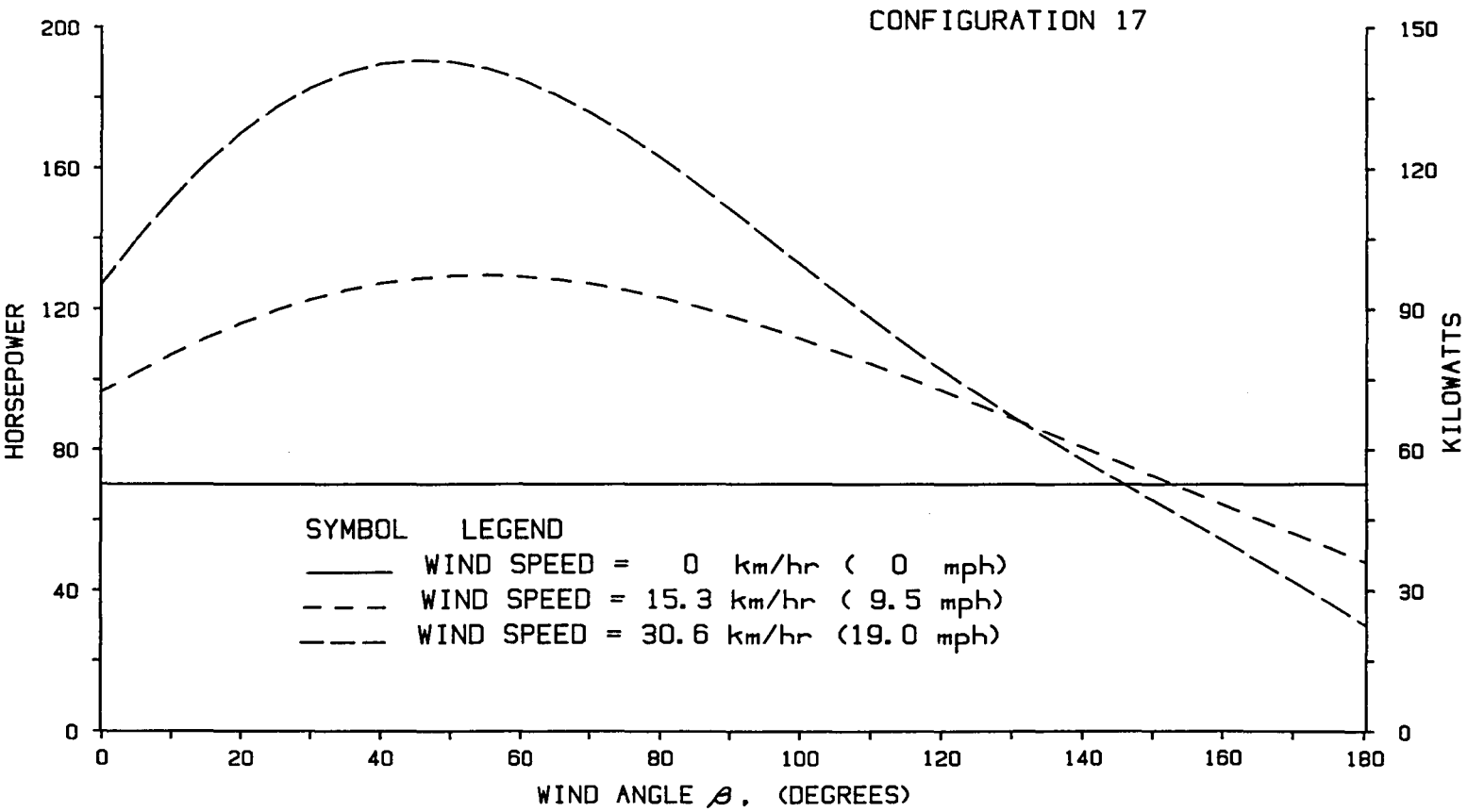

FIGURE 3.1.16 POWER REQUIRED TO OVERCOME AERODYNAMIC DRAG, CONFIGURATION 17

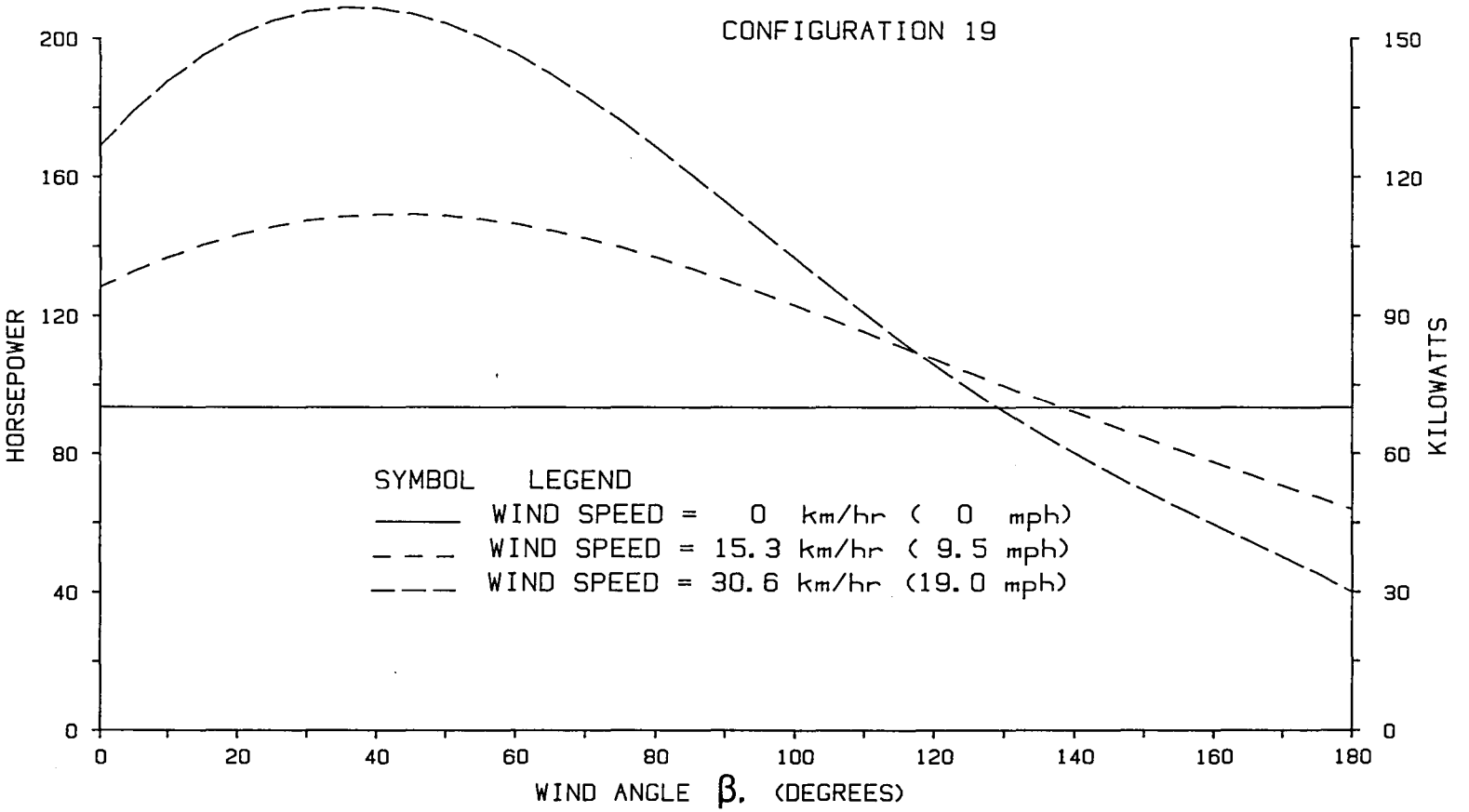

FIGURE 3.1.17 POWER REQUIRED TO OVERCOME AERODYNAMIC DRAG, CONFIGURATION 19

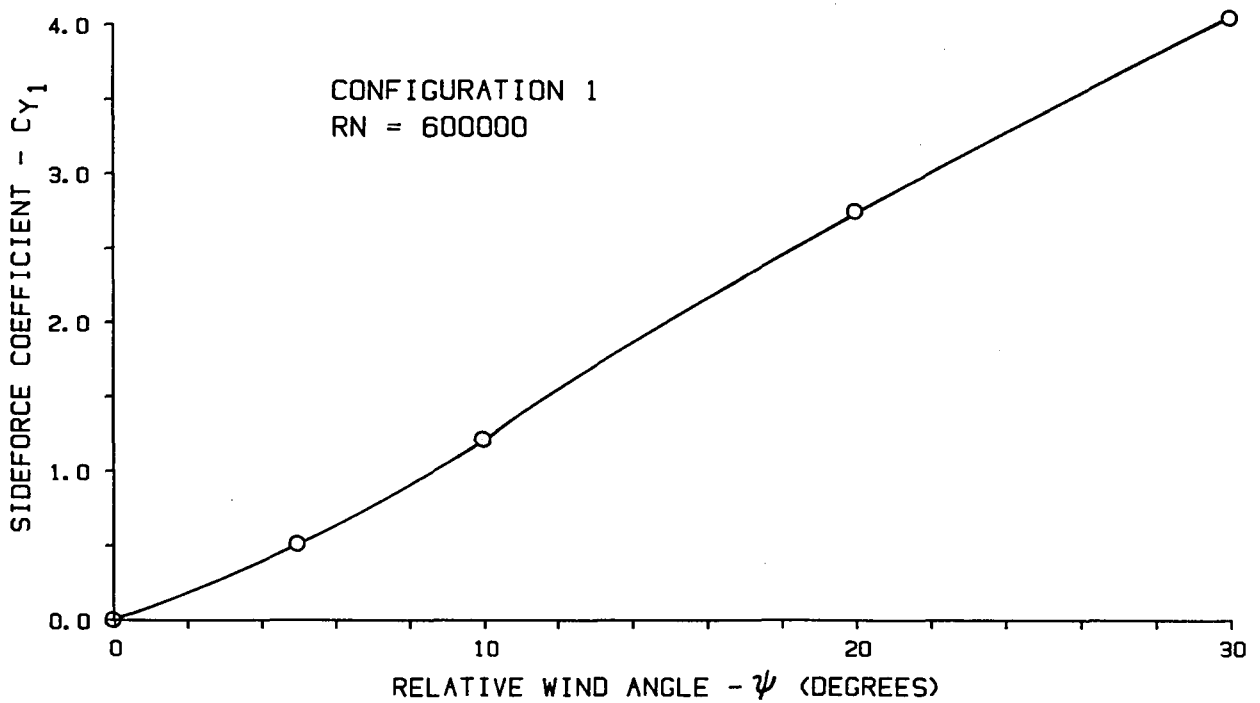

FIGURE 3.2.1 EFFECT OF RELATIVE WIND ANGLE ON SIDE FORCE COEFFICIENT C_{Y_1}

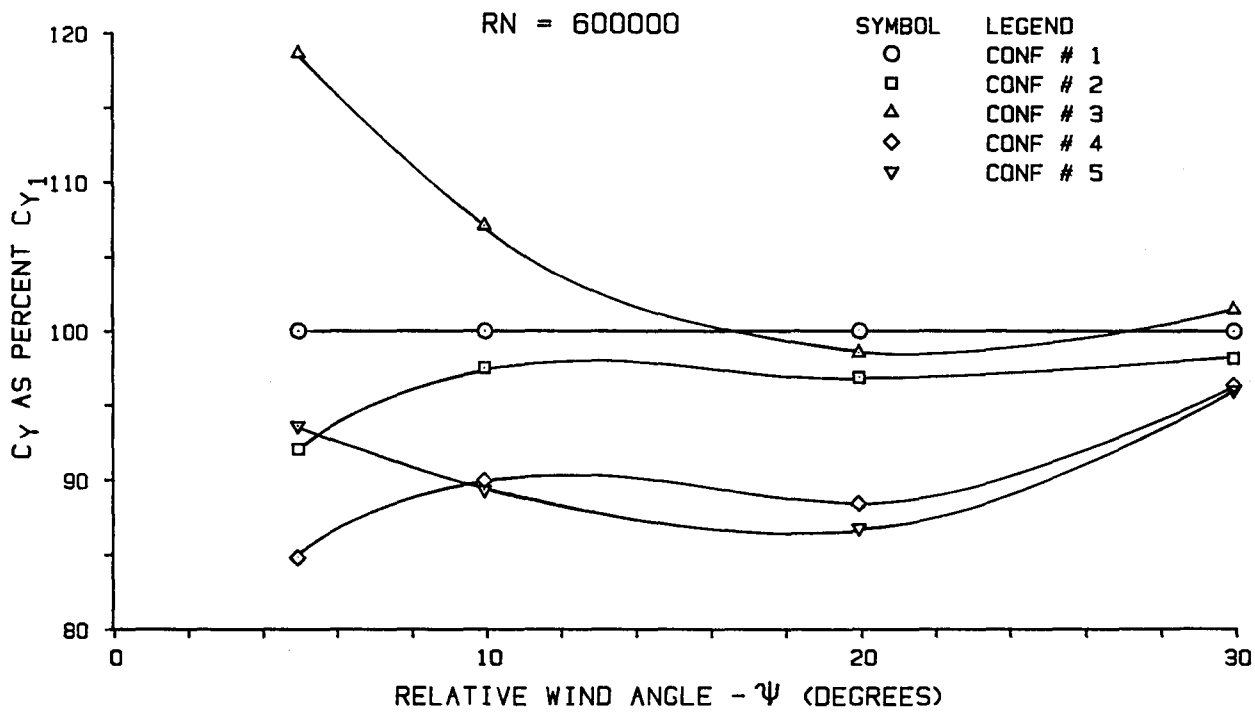

FIGURE 3.2.2 COMPARISON OF SIDE FORCE COEFFICIENTS, CONFIGURATIONS 1, 2, 3, 4, 5

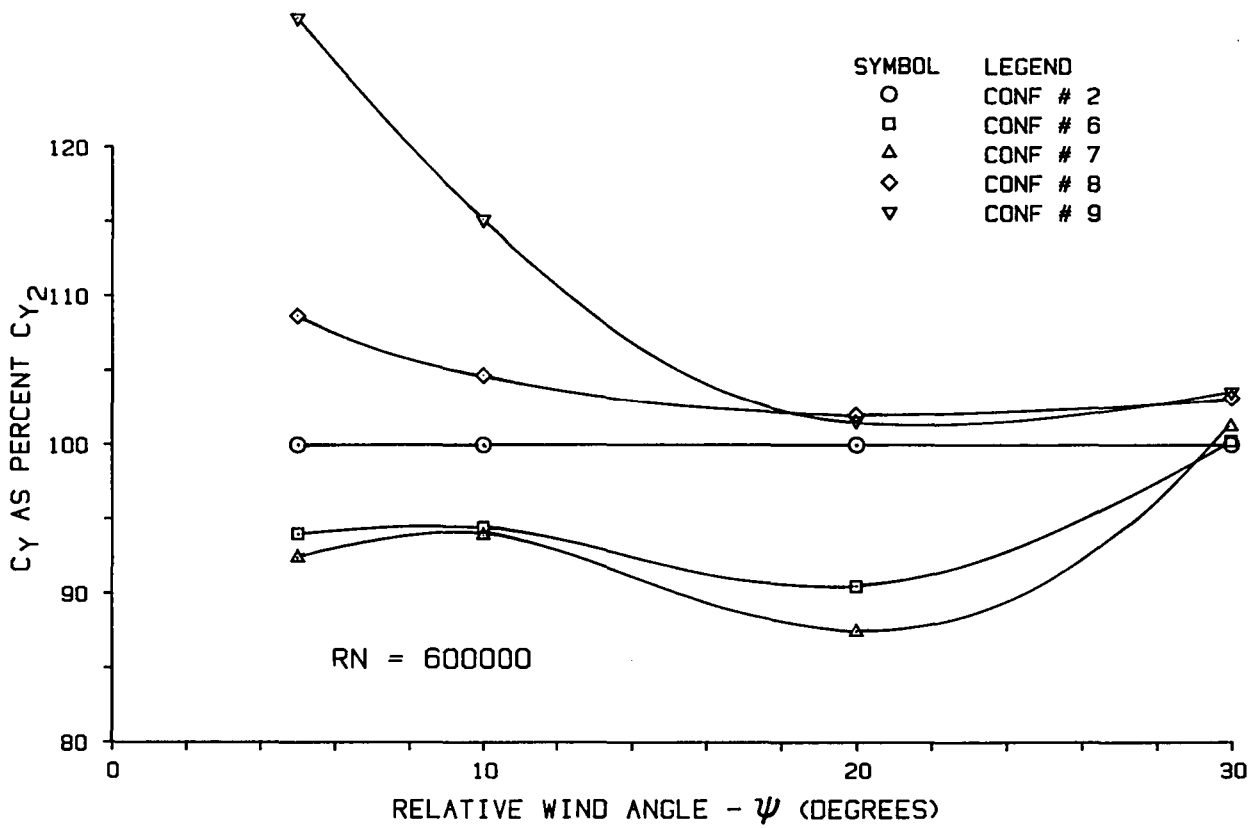

FIGURE 3.2.3 COMPARISON OF SIDE FORCE COEFFICIENTS, CONFIGURATIONS 2, 6, 7, 8, 9

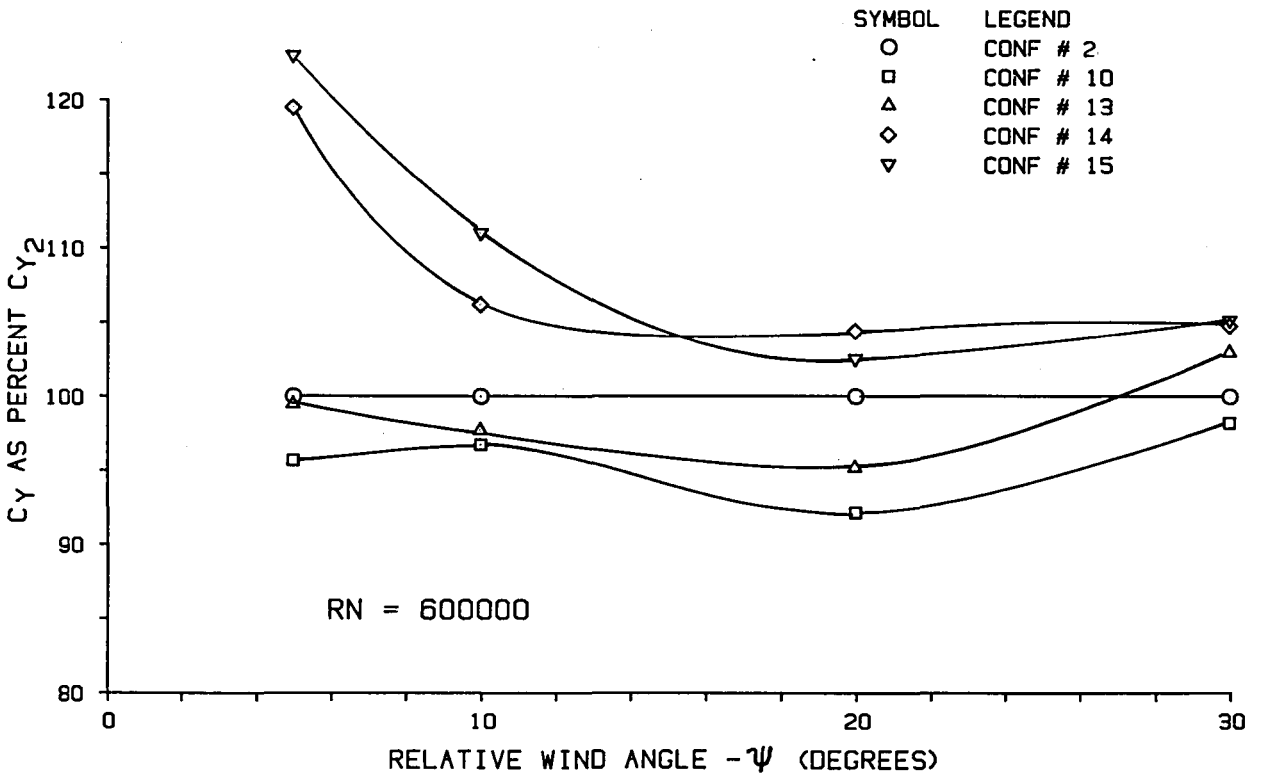

FIGURE 3.2.4 COMPARISON OF SIDE FORCE COEFFICIENTS, CONFIGURATIONS 2, 10, 13, 14, 15

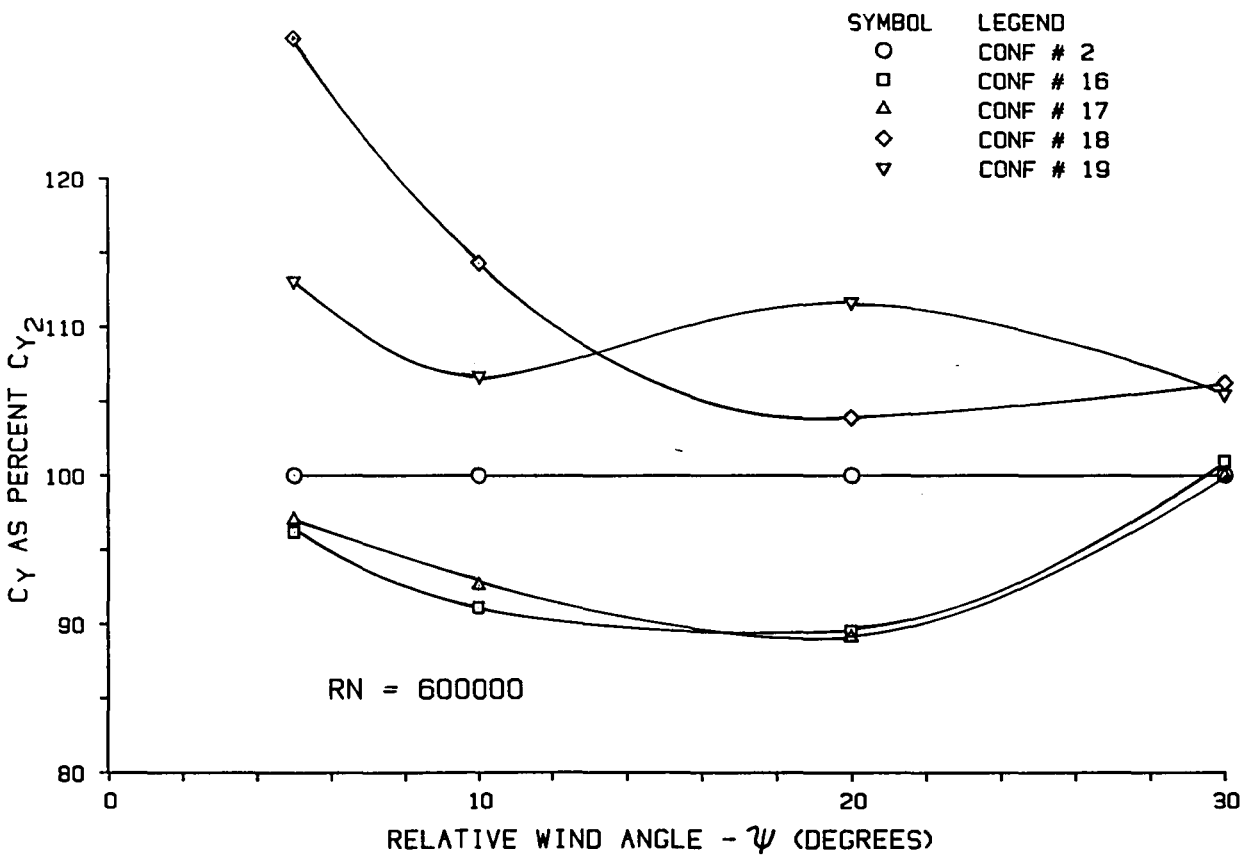

FIGURE 3.2.5 COMPARISON OF SIDE FORCE COEFFICIENTS, CONFIGURATIONS 2, 16, 17, 18, 19

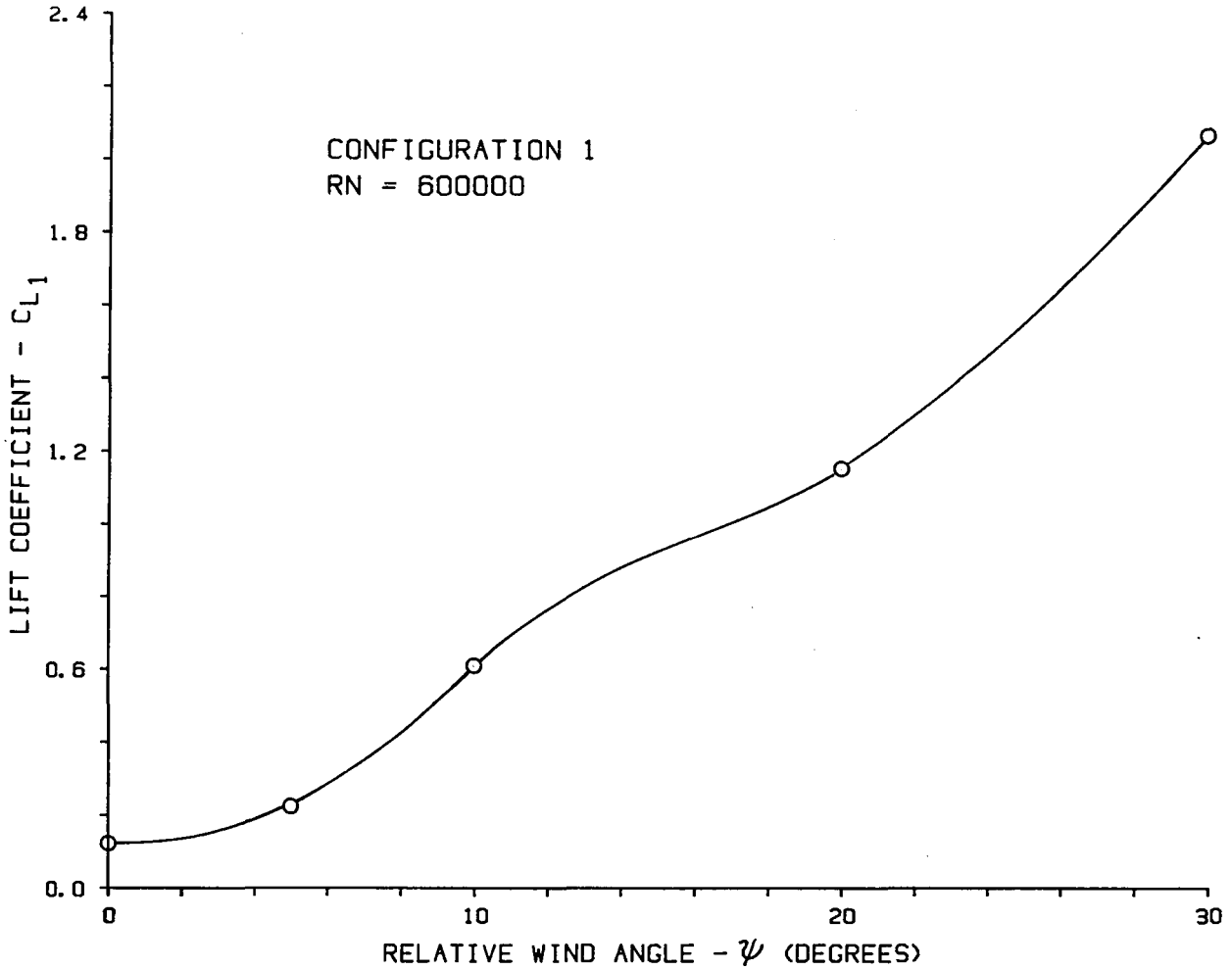

FIGURE 3.3.1 EFFECT OF RELATIVE WIND ANGLE ON LIFT COEFFICIENT C_{L_1}

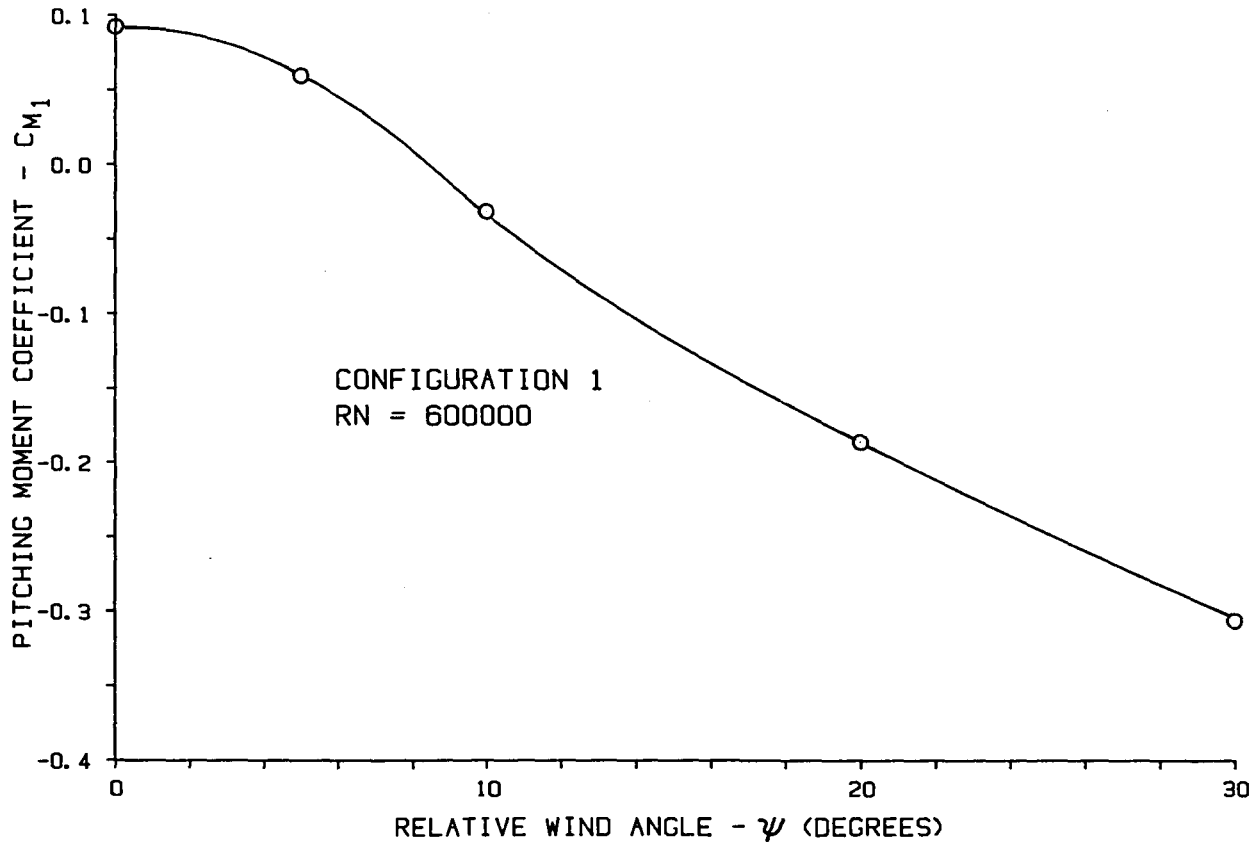

FIGURE 3.4.1 EFFECT OF RELATIVE WIND ANGLE ON PITCHING MOMENT COEFFICIENT C_{M_1}

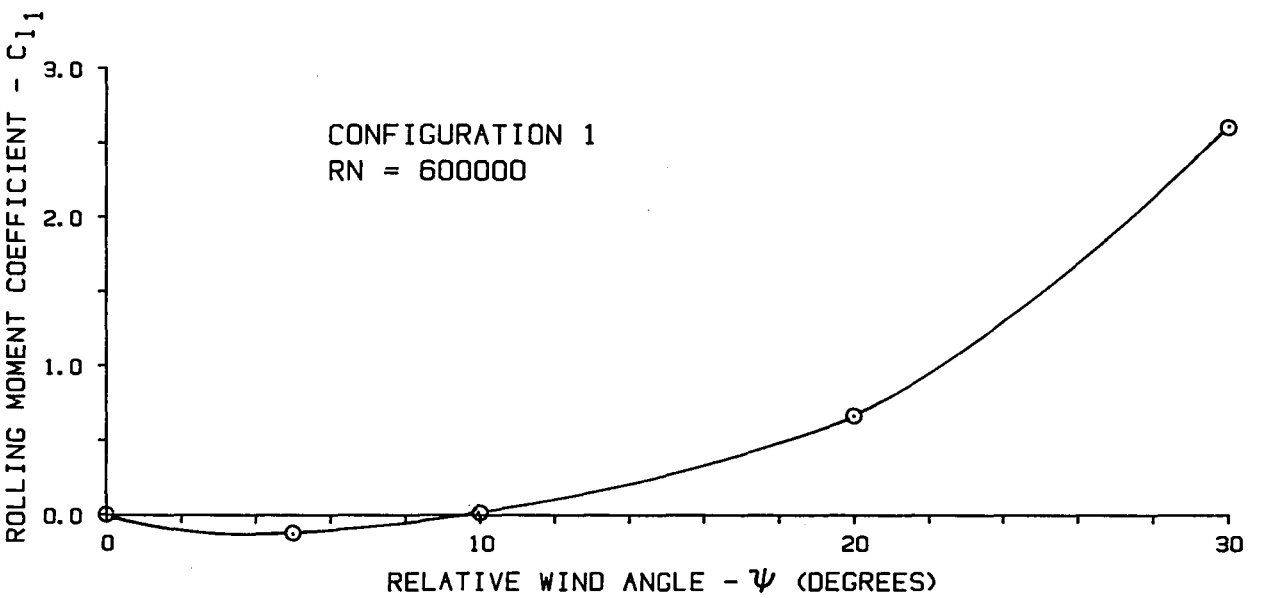

FIGURE 3.5.1 EFFECT OF RELATIVE WIND ANGLE ON ROLLING MOMENT COEFFICIENT C_{l_1}

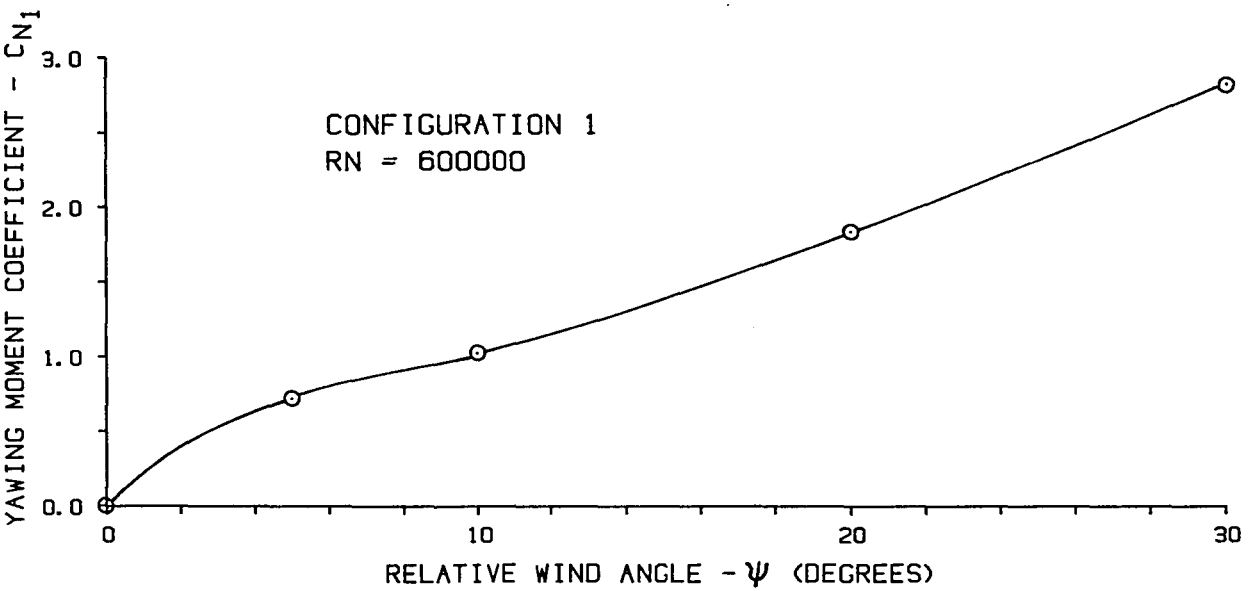

FIGURE 3.6.1 EFFECT OF RELATIVE WIND ANGLE ON YAWING MOMENT COEFFICIENT C_{N_1}

Table I Full-scale basic vehicle characteristics

Tractor:	
Make	White Freightliner
Year	1974
Type	Cab over engine (with sleeper)
Number of axles	3
Tire size	10.00-22
Engine:	
Type	350 Cummins Turbocharged
Model	NTC-350
Displacement, in^3	855
Horsepower at 2100 rpm	310
Transmission:	
Type	Fuller Roadranger
Model	RTO-9513
Trailer:	
Make	Strick
Year	1972
Length, ft	45
Type	Smooth sidewall
Number of axles	2
Tire size	10.00-22

Table II Drag coefficients, $R_N = 6 \times 10^5$

Configuration Number	Yaw angles, ψ 0	5	10	20	30	Avg (0 to 10)	Avg (0 to20)
1	0.946	1.081	1.332	1.639	1.686	1.120	1.250
2	0.952	1.063	1.346	1.656	1.696	1.120	1.254
3	0.758	1.019	1.324	1.625	1.691	1.034	1.182
4	0.895	1.003	1.229	1.555	1.612	1.042	1.171
5	0.700	0.946	1.227	1.518	1.622	0.958	1.098
6	0.902	1.009	1.318	1.736	1.799	1.076	1.241
7	0.944	1.027	1.340	1.720	1.818	1.104	1.258
8	0.938	1.060	1.418	1.793	1.879	1.139	1.302
9	0.739	1.000	1.359	1.755	1.864	1.033	1.213
10	0.894	0.990	1.233	1.559	1.633	1.039	1.169
11	0.599	0.637	0.747	0.855	0.900	0.661	0.710
12	0.830	0.842	0.932	0.999	1.009	0.868	0.901
13	0.905	0.949	1.198	1.533	1.606	1.017	1.146
14	0.955	1.010	1.273	1.606	1.679	1.079	1.211
15	0.697	0.920	1.218	1.574	1.714	0.945	1.102
16	0.668	0.872	1.159	1.548	1.683	0.900	1.062
17	0.667	0.877	1.140	1.398	1.500	0.895	1.020
18	0.713	0.988	1.271	1.510	1.596	0.991	1.120
19	0.892	1.018	1.274	1.429	1.614	1.061	1.153

Table III Influence on drag coefficient of configuration changes and relative wind angles

CONFIGURATION		DRAG	
Parts Added	No. to No.	Zero wind[1] incremental change	Average wind[2] incremental change
Transition	1 → 2	+ 0.6%	+ 0.3%
Device "A"	1 → 3	-19.9%	- 5.4%
Boattail	1 → 4	- 5.4%	- 6.3%
Device "A" & Boattail	1 → 5	-26.0%	-12.2%
Transition small Flow-Vane, Boattail:	2 → 6	- 5.2%	- 1.0%
Transition small Flow-Vane, Chopped Boattail:	2 → 7	- 0.8%	+ 0.3%
Transition small Flow-Vane:	2 → 8	- 1.5%	+ 3.8%
Transition small Flow-Vane Device "A":	2 → 9	-22.4%	- 3.3%
Transition, Boattail:	2 → 10	- 6.1%	- 6.8%
Transition, Flow-Vane, Boattail:	2 → 13	- 4.9%	- 8.6%
Transition, Flow-Vane:	2 → 14	+ 0.3%	- 3.4%
Transition, Flow-Vane, Device "A", Boattail:	2 → 15	-26.8%	-12.1%
Device "A", Flow-Vane, Boattail:	2 → 16	-29.8%	-15.3%
Device "A", Small gap, Boattail:	2 → 17	-29.9%	-18.7%
Device "A", Small gap:	2 → 18	-25.1%	-10.7%
Small gap:	2 → 19	- 6.3%	- 8.1%
Cab Only	1 → 11	-36.7%	-43.2%
Cab Only Device "A"	1 → 12	-12.3%	-27.9%

Note: 1. $R_N = 6 \times 10^5$

2. Qualitative-relative winds from $\psi = 0°$ to $\psi = 20°$

Table IV Drag increments provided by the two most promising modifications

Modification	Configuration Comparison	1, 3 Zero Wind Delta	1, 3 Average Wind Delta,[2]
Cab mounted Deflector	1 → 3	-19.9%	- 5.4%
	4 → 5	-20.6%	- 5.8%
	13 → 16	-24.9%	- 6.7%
	19 → 18	-18.8%	- 2.6%
Boattail	1 → 4	- 5.4%	- 6.3%
	3 → 5	- 6.1%	- 6.7%
	2 → 10	- 6.1%	- 6.8%
	14 → 13	- 5.2%	- 5.2%
	15 → 16	- 3.0%	- 3.2%
	18 → 17	- 4.8%	- 8.0%

Note: 1. $R_N = 6 \times 10^5$

2. Qualitative-relative winds from $\psi = 0°$ to ψ 20°

3. Drag increment percentages from configurations having forced transition normalized by configuration 2 and drag increment percentage from configurations without forced transition normalized by configuration 1.

Table V Comparison of tests run at Dryden Flight Research Center and the University of Kansas

Configuration Identification			Drag Coefficients		Difference	
DFRC	KU		DFRC	KU	ΔC_D	%
Baseline	1		1.17	.946	-.224	-19.1
62" gap	2		1.17	.952	-.218	-18.6
Baseline 62" with Device "A"	3		.89	.758	-.132	-14.8
Baseline 40"gap	19		1.06	.892	-.168	-15.8
Baseline 40" with Device "A"	18		.89	.713	-.177	-19.9
Device A	1 → 3	ΔC_D	-.28	-.188		
		%	-23.9	-19.9		
	19 → 18	ΔC_D	-.17	-.179		
		%	-16.0	-20.1		
40" gap	2 → 19	ΔC_D	-0.11	-.060		
		%	-9.4	-6.3		

Note: 1. All data at $\beta = 0°$.

2. DFRC data from References 2, 3 and 6.

3. Reference 5 baseline 62" gap C_D = .990, see Section 3.1, page 4.

Table VI Base Pressure coefficients $R_N = 6 \times 10^5$

Configuration Number	Yaw Angle, ψ 0	5	10	20	30
1	-0.214	-0.359	-0.529	-0.590	-0.801
2	-0.211	-0.346	-0.532	-0.588	-0.831
3	-0.212	-0.303	-0.418	-0.613	-0.795
4	-0.013	-0.027	-0.074	-0.317	-0.602
5	-0.022	-0.054	-0.100	-0.266	-0.579
6	-0.053	-0.109	-0.172	-0.397	-0.616
7	-0.108	-0.089	-0.109	-0.305	-0.589
8	-0.196	-0.314	-0.492	-0.570	-0.810
9	-0.199	-0.287	-0.379	-0.579	-0.803
10	-0.023	-0.032	-0.062	-0.333	-0.606
13	-0.002	-0.043	-0.056	-0.368	-0.629
14	-0.229	-0.328	-0.493	-0.598	-0.865
15	-0.186	-0.284	-0.402	-0.592	-0.891
16	-0.027	-0.050	-0.082	-0.355	-0.593
17	-0.021	-0.037	-0.045	-0.397	-0.592
18	-0.182	-0.289	-0.435	-0.575	-0.804
19	-0.216	-0.348	-0.514	-0.656	-0.786

Table VII Average power required to overcome aerodynamic drag for all configurations tested

Configuration Number	Wind Speed km/hr(mph)		
	0	15.3(9.5)	30.6(19.0)
1	75(100)	94(125)	115(154)
2	75(100)	93(125)	115(155)
3	60(80)	89(119)	112(150)
4	71(95)	87(116)	107(144)
5	55(74)	82(111)	104(139)
6	71(95)	90(120)	116(155)
7	74(99)	92(123)	116(156)
8	73(98)	95(128)	121(163)
9	58(78)	89(119)	116(156)
10	70(94)	86(116)	107(144)
11	47(63)	54(73)	63(85)
12	66(88)	71(95)	78(105)
13	71(95)	84(112)	105(140)
14	75(100)	89(119)	111(148)
15	55(73)	81(109)	105(140)
16	53(70)	77(103)	101(136)
17	52 (70)	77(103)	96(129)
18	56(75)	86(115)	106(142)
19	70(93)	89(119)	105(141)

Note: 1. Ground speed = 88.6 km/hr(55mph).

2. Power values are integrated over wind angles from 0° to 180°.

3. Power value units, KW (HP)

Table VIII Average fuel consumption per hour required to overcome aerodynamic drag for all configurations tested

Configuration Number	Fuel Consumption liters/hr(gal/hr)	Fuel Savings liters/hr(gal/hr)	% Saving*	Cost Savings $/hr
1	23.9(6.4)	0.0(0.0)	0	0.00
2	23.8(6.3)	0.0(0.0)	0	0.00
3	22.7(6.0)	1.2(0.4)	5	0.40
4	22.1(5.9)	1.8(0.5)	7	0.50
5	21.0(5.6)	2.9(0.8)	12	0.80
6	22.9(6.1)	0.9(0.2)	4	0.20
7	23.4(6.2)	0.4(0.1)	2	0.10
8	24.3(6.5)	-0.5(-0.2)	-2	-0.20
9	22.7(6.1)	1.1(0.2)	5	0.20
10	22.0(5.9)	1.8(0.4)	8	0.40
11	13.9(3.7)			
12	18.1(4.8)			
13	21.4(5.7)	2.4(0.6)	10	0.60
14	22.7(6.1)	1.1(0.2)	5	0.20
15	20.7(5.5)	3.1(0.8)	13	0.80
16	19.6(5.2)	4.2(1.1)	18	1.10
17	19.6(5.2)	4.2(1.1)	18	1.10
18	21.9(5.8)	1.9(0.2)	8	0.50
19	22.7(6.1)	1.1(0.2)	5	0.20

Note:
1. Ground speed = 88.6 km/hr (55mph)
2. Wind speed = 15.3 km/hr(9.5mph)
3. BSFC = .2129 kg/kw-hr(.3511 lbs/hp-hr)
4. Fuel cost = $0.264/liter($1.00/gal)
5. *percent saving of aerodynamic drag portion of fuel budget, not percent saving of total fuel budget

Table IX Side force coefficients, $R_N = 6 \times 10^5$

Configuration Number	Yaw Angles, ψ				
	0	5	10	20	30
1	0.000	0.512	1.211	2.751	4.052
2	0.000	0.471	1.181	2.665	3.978
3	0.000	0.607	1.296	2.710	4.111
4	0.000	0.434	1.089	2.432	3.905
5	0.000	0.479	1.081	2.386	3.891
6	0.000	0.443	1.115	2.411	3.988
7	0.000	0.436	1.109	2.329	4.026
8	0.000	0.512	1.236	2.718	4.104
9	0.000	0.607	1.360	2.708	4.120
10	0.000	0.451	1.143	2.455	3.907
11	0.000	0.044	0.234	0.441	0.577
12	0.000	0.064	0.122	0.224	0.456
13	0.000	0.469	1.154	2.536	4.096
14	0.000	0.563	1.254	2.782	4.169
15	0.000	0.580	1.311	2.732	4.184
16	0.000	0.454	1.076	2.386	4.015
17	0.000	0.457	1.094	2.374	3.976
18	0.000	0.610	1.350	2.769	4.226
19	0.000	0.533	1.261	2.976	4.197

Table X Lift coefficient, $R_N = 6 \times 10^5$

Configuration Number	Yaw Angles, ψ				
	0	5	10	20	30
1	0.121	0.223	0.609	1.152	2.067
2	0.141	0.260	0.641	1.207	2.053
3	-0.013	-0.018	0.122	0.822	1.846
4	0.308	0.393	0.814	1.377	2.320
5	0.050	0.101	0.273	1.014	2.159
6	0.258	0.329	0.566	1.347	2.325
7	0.326	0.406	0.606	1.363	2.316
8	0.144	0.179	0.387	1.106	2.043
9	-0.030	0.018	0.153	0.800	1.867
10	0.274	0.408	0.810	1.410	2.312
11	0.154	0.164	0.216	0.262	0.279
12	-0.070	-0.070	-0.056	-0.017	0.049
13	0.251	0.374	0.650	1.354	2.365
14	0.158	0.205	0.425	1.023	2.090
15	-0.030	0.001	0.195	0.917	2.039
16	0.089	0.127	0.326	1.145	2.229
17	0.094	0.133	0.348	1.203	2.152
18	-0.031	0.003	0.163	0.794	1.909
19	-0.111	-0.212	-0.535	-1.523	-2.165

Table XI Pitching moment coefficients
$R_N = 6 \times 10^5$

Configuration Number	Yaw Angles, ψ				
	0	5	10	20	30
1	0.092	0.059	-0.031	-0.186	-0.306
2	0.085	0.061	-0.034	-0.179	-0.304
3	-0.037	-0.080	-0.137	-0.273	-0.349
4	0.021	-0.024	-0.139	-0.293	-0.375
5	-0.096	-0.145	-0.217	-0.375	-0.416
6	0.018	-0.018	-0.113	-0.292	-0.365
7	-0.005	-0.038	-0.118	-0.316	-0.377
8	0.082	0.059	-0.024	-0.178	-0.300
9	-0.035	-0.072	-0.135	-0.253	-0.335
10	0.024	-0.021	-0.141	-0.299	-0.372
11	-0.002	-0.003	0.000	-0.033	-0.099
12	-0.077	-0.073	-0.058	-0.052	-0.052
13	0.024	-0.009	-0.113	-0.299	-0.369
14	0.095	0.078	-0.005	-0.170	-0.301
15	-0.038	-0.082	-0.144	-0.272	-0.349
16	-0.095	-0.139	-0.217	-0.393	-0.401
17	-0.095	-0.138	-0.215	-0.389	-0.396
18	-0.032	-0.076	-0.131	-0.256	-0.336
19	0.079	0.058	-0.026	-0.199	-0.299

Table XII Rolling moment coefficients

$R_N = 6 \times 10^5$

Configuration Number	Yaw Angles, ψ				
	0	5	10	20	30
1	0.000	-0.122	0.014	0.664	2.609
2	0.000	-0.138	0.001	0.724	2.561
3	0.000	0.007	0.158	1.148	3.903
4	0.000	-0.006	0.299	1.322	3.538
5	0.000	0.107	0.401	1.824	4.052
6	0.000	-0.008	0.183	1.385	3.474
7	0.000	-0.099	0.009	1.160	2.883
8	0.000	-0.148	-0.104	0.630	2.575
9	0.000	-0.006	0.148	1.058	3.007
10	0.000	-0.019	0.301	1.364	3.416
11	0.000	-0.015	-0.048	-0.207	-0.479
12	0.000	-0.690	-0.663	-0.649	-0.632
13	0.000	-0.070	0.185	1.401	3.501
14	0.000	-0.168	-0.124	0.592	2.650
15	0.000	0.010	0.201	1.189	3.175
16	0.000	0.117	0.430	1.958	3.862
17	0.000	0.108	0.410	1.904	3.656
18	0.000	0.005	0.153	1.033	2.982
19	0.000	-0.141	-0.032	0.944	2.537

Table XIII Yawing moment coefficients

$R_N = 6 \times 10^5$

Configuration Number	Yaw Angles, ψ				
	0	5	10	20	30
1	0.000	0.723	1.024	1.837	2.827
2	0.000	0.788	1.150	1.936	2.891
3	0.000	1.070	1.458	2.156	3.121
4	0.000	0.503	0.692	0.866	2.464
5	0.000	0.657	0.787	1.251	2.483
6	0.000	0.273	1.108	1.154	2.274
7	0.000	0.449	1.263	1.342	2.480
8	0.000	0.598	1.648	2.208	2.706
9	0.000	1.121	1.639	2.353	3.012
10	0.000	0.526	0.753	0.978	2.518
11	0.000	0.047	0.089	-0.514	-1.830
12	0.000	0.053	-0.172	-0.520	-1.010
13	0.000	0.265	0.763	0.900	2.200
14	0.000	0.589	1.285	1.933	2.654
15	0.000	0.965	1.284	1.865	2.786
16	0.000	0.420	0.532	0.781	2.192
17	0.000	0.607	0.774	0.820	2.376
18	0.000	0.957	1.315	1.846	2.732
19	0.000	0.501	0.829	1.011	2.469

7. APPENDIX

POWER REQUIRED

The model data for Configuration 1 were applied to the full size prototype vehicle at road speed of 88.5 km/hr (55 mph). The wind component was rotated from 0° to 180°. Wind speeds used were 0, 15.3 km/hr (9.5 mph), 30.6 km/hr (19.0 mph).

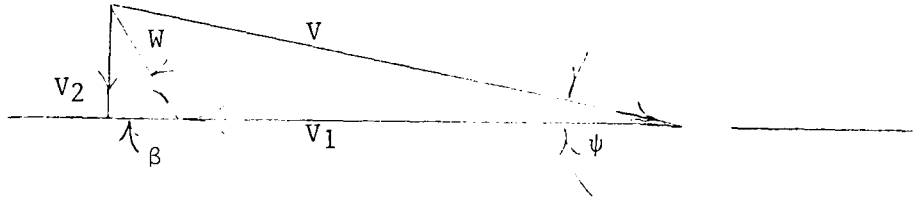

V = Relative wind speed

V_1 = Ground speed

W = Actual wind velocity

V_2 = Side wind velocity component

β = Wind angle relative to the vehicle path

ψ = Relative wind angle

7.1 Power to Overcome Aerodynamic Drag - Configuration 1

The power required is:

$$P = \frac{D\ V_1}{1000} \text{ kw (Multiply by 1.341 = hp)}$$

where

$$D = 1/2\ \rho V^2 C_D A$$

$A = 8.724\ m^2$ (94 ft^2)

$\rho = 1.226\ kg/m^3$ (.002378 $slugs/ft^3$)

C_D is taken from Figure 3.1.1 for Configuration 1 at approximate values of ψ.

Example:

V_1 = 88.5 km/hr or 24.58 m/sec (55 mph)

W = 15.3 km/hr or 4.25 m/sec (9.5 mph)

$\beta = 15°$

$\psi = 2.19°$

From Figure 3.1.1:

$$C_{D_1} = 1.00$$

Then:

$$D = 1/2 \times 1.226 \times (28.71)^2\ (1.00)\ (8.724)$$

$$D = 4408.0\ N$$

$$P = \frac{(4408.0)(24.58)}{1000} = 108.3\ kw$$

$$P = 108.3\ (145.3\ hp)$$

7.2 Power Required for Other Configurations

To find the power required for any other configuration:

1. Determine relative wind speed V and the relative wind angle ψ.
2. Go to Figures 3.1.2, 3.1.3, 3.1.4, 3.1.5, 3.1.6. Find the

percentage of C_{D_X} this configuration has of C_{D_1} or C_{D_2}, depending on configuration used for normalizing.

3. Go to the power graph, Figure 3.1.12, and locate the power required for Configuration 1 at the wind angle β (for Configuration 6 to 10 and 13 to 19 use the power curves for configuration 2).
4. Multiply this value of power with C_{D_X}/C_{D_1} (or C_{D_X}/C_{D_2} for appropriate configuration) and the power required for this configuration X is obtained.

Example:

1. Configuration 5

Wind speed W = 15.3 km/hr (9.5 mph)

Wind angle $\beta = 15°$

Relative wind angle :

$$\psi = \text{Tan}^{-1} \frac{W \sin\beta}{V_1 + W \cos\beta}$$

$$\psi = \text{Tan}^{-1} \frac{15.3 \text{ km/hr} \sin 15^0}{88.5 \text{ km/hr} + 15.3 \text{ km/hr} \cos 15^0}$$

$$\psi = 2.19^0$$

From Figure 3.1.2 or 3.1.6 where C_{D_1} is the normalizing coefficient (use Figures 3.1.3, 3.1.4, 3.1.5 where C_{D_2} is the normalizing coefficient).

$$\frac{C_{D_5}}{C_{D_1}} = 81.3\% = \frac{P_5}{P_1}$$

From Figure 3.1.12:

P_1 = 108.3 kw (145.3 hp) and P_5 = 88.0 kw (118.1 hp)

1. Report No.	2. Government Accession No.	3. Recipient's Catalog No.
CR-163104		

4. Title and Subtitle	5. Report Date
An Investigation of Drag Reduction for Tractor Trailer Vehicles with Air Deflector and Boattail	January 1981
	6. Performing Organization Code 141-20-11
7. Author(s)	8. Performing Organization Report No.
Vincent U. Muirhead	KU-FRL 406-1
	10. Work Unit No.
9. Performing Organization Name and Address	
University of Kansas Center for Research, Incorporated 2291 Irving Hill Drive--Campus West Lawrence, Kansas 66045	11. Contract or Grant No. NSG 4021 and 4023
	13. Type of Report and Period Covered Contractor Report - Final
12. Sponsoring Agency Name and Address	
National Aeronautics and Space Administration Washington, DC 20546	14. Sponsoring Agency Code

15. Supplementary Notes

NASA Technical Monitor: Edwin J. Saltzman, Dryden Flight Research Center

16. Abstract

A wind tunnel investigation was conducted to determine the influence of several physical variables on the aerodynamic drag of a tractor-trailer model. The physical variables included: a cab mounted wind deflector, boattail on trailer, flow vanes on trailer front, forced transition on trailer, and decreased gap between tractor and trailer. Tests were conducted at yaw angles (relative wind angles) of 0, 5, 10, 20, and 30 degrees and Reynolds numbers of 3.58×10^5 to 6.12×10^5 based upon the equivalent diameter of the vehicles.

The wind deflector on top of the cab produced a calculated reduction in fuel consumption of about 5% of the aerodynamic portion of the fuel budget for a wind speed of 15.3 km/hr (9.5 mph) over a wind angle range of 0° to 180° and for a vehicle speed of 88.5 km/hr (55 mph). The boattail produced a calculated 7% to 8% reduction in fuel consumption under the same conditions. The decrease in gap reduced the calculated fuel consumption by about 5% of the aerodynamic portion of the fuel budget.

17. Key Words (Suggested by Author(s))	18. Distribution Statement
Aerodynamic drag Streamlining Fuel economy	Unclassified - Unlimited Subject category 85

19. Security Classif. (of this report)	20. Security Classif. (of this page)	21. No. of Pages	22. Price*
Unclassified	Unclassified	68	$7.00

For sale by the National Technical Information Service, Springfield, Virginia 22161

End of Document